BNL- 66103
INFORMAL REPORT

THERMALLY CONDUCTIVE CEMENTITIOUS GROUTS FOR GEOTHERMAL HEAT PUMPS

PROGRESS REPORT FY 1998

M.L. Allan and A.J. Philippacopoulos

November 1998

Prepared for:
Office of Geothermal Technologies
United States Department of Energy
Washington, DC 20585

DEPARTMENT OF APPLIED SCIENCE
Energy Efficiency and
Conservation Division
BROOKHAVEN NATIONAL LABORATORY
UPTON, LONG ISLAND, NEW YORK 11973

BNL-66103
Informal Report

THERMALLY CONDUCTIVE CEMENTITIOUS GROUTS FOR GEOTHERMAL HEAT PUMPS: PROGRESS REPORT FY 98

M.L. ALLAN and A.J. PHILIPPACOPOULOS

NOVEMBER 1998

Prepared for:
Office of Geothermal Technologies
U.S. Department of Energy
1000 Independence Ave., S.W.
Washington, D.C. 20585

Energy Efficiency and Conservation Division
Department of Applied Science
Brookhaven National Laboratory
Upton, New York 11973-5000

This work was performed under the auspices of the U.S. Department of Energy, Washington, D.C., under Contract No. DE-AC02-98CH10886.

DISCLAIMER

DISCLAIMER

Portions of this document may be illegible in electronic image products. Images are produced from the best available original document.

CONTENTS

SUMMARY

Research commenced in FY 97 to determine the suitability of superplasticized cement-sand grouts for backfilling vertical boreholes used with geothermal heat pump (GHP) systems. The overall objectives were to develop, evaluate and demonstrate cementitious grouts that could reduce the required bore length and improve the performance of GHPs. This report summarizes the accomplishments in FY 98.

The developed thermally conductive grout consists of cement, water, a particular grade of silica sand, superplasticizer and a small amount of bentonite. In order to simplify field mixing, the grout formulation was changed in FY 98 to use two 100 lb bags of sand to one 94 lb bag of cement. The thermal conductivity of the re-formulated grout (Mix 111, a.k.a. Bonus Grout) was 2.42 W/m.K (1.40 Btu/hr.ft.°F) when wet cured. Slightly lower values are obtained when the grout is cured under sealed conditions. The cement-sand grout is approximately three times more conductive than conventional high solids bentonite and neat cement (cement plus water only) grouts. The thermal conductivity is approximately 1.6 times greater than that for thermally enhanced bentonite. Another benefit of the cement-sand grout is good retention of thermal conductivity under drying conditions and the value decreased to 2.16 W/m.K (1.25 Btu/hr.ft.°F) when oven dried.

Mix 111 has been designed to meet a balance between required properties, economics and ease of use with conventional geotechnical grouting equipment. Its components are readily available throughout the U.S. Specifications for mixing and placement are included in this report. Alternatively, the dry ingredients could be preblended and prepackaged so that the GHP contractor only needs to add water. The estimated material cost of Mix 111 is 16.1 c/litre (60.8 c/U.S. gallon) if the ingredients are purchased separately. Previous analysis conducted by the University of Alabama in FY 97 on cement-sand grouts with similar thermal conductivities suggest theoretical bore length reductions of 22 to 37% compared with neat cement grout having a thermal conductivity of 0.84 W/m.K. Therefore, in addition to the relatively low material cost, the proposed grout/backfill offers significant potential savings in installation costs due to reduced bore lengths.

While the primary function of the grout is to facilitate heat transfer between the U-loop and surrounding formation, it is also essential that the grout act as an effective borehole sealant. The latter role is important to prevent leakage of surface contaminants to aquifers or cross contamination between aquifers. Studies of the interfacial bonding showed that gaps between Mix 111 grout and U-loop were variable, discontinuous and 0.025 to 0.075 mm (9.8×10^{-4} to 2.9×10^{-3} in.) wide.

Two types of permeability (hydraulic conductivity) tests were conducted to evaluate the sealing performance of the cement-sand grout. The first of these considered the bulk grout and the coefficient of permeability was determined to be of the order of 10^{-10} cm/s. Hydraulic conductivity of the grout/U-loop system was measured on grout cast around two vertically oriented high density polyethylene (HDPE) pipes. This test arrangement simulated a grouted borehole and took into account potential flow at the grout/pipe interfaces. The results clearly demonstrated that cement-sand

grouts possess significantly lower system coefficient of permeability and better bonding to HDPE than neat cement grouts over a range of representative temperatures. For example, the system coefficient of permeability of Mix 111 was of the order of 10^{-7} cm/s at 21°C compared with 10^{-6} to 10^{-5} cm/s for neat cement systems. Coefficient of permeability of Mix 111/pipe specimens increased slightly after wet-dry or thermal cycles but remained of the order of 10^{-7} cm/s. In contrast, neat cement grouts cracked when subjected to the same cycles and therefore lack the required durability.

Additional properties of the proposed grout that were investigated include bleeding, shrinkage, bond strength, freeze-thaw durability, compressive, flexural and tensile strengths, elastic modulus, Poisson's ratio and ultrasonic pulse velocity. The University of Alabama conducted thermal resistance tests on grouted tubes.

BNL has received numerous expressions of interest from the GHP industry in using the thermally conductive cement-sand grout, particularly in states where neat cement or bentonite grouts are not permitted due to environmental concerns. We have also interacted with the New Jersey Heat Pump Council and New Jersey Department of Environmental Protection to help resolve the temporary injunction on installation of ground heat exchangers in consolidated formations due to lack of confidence in the sealing ability of neat cements.

The first field trial of the superplasticized cement-sand grout was conducted at Oklahoma State University (OSU) and the second at Sandia National Laboratories (SNL). Two 250 ft deep boreholes were grouted at OSU. Following the field trial at OSU, the grout mix was altered to include a small proportion of bentonite to improve grout stability. The grout containing bentonite was successfully mixed and pumped at SNL and used to complete two 250 ft boreholes. The boreholes will be used to assess the thermal performance of the cement-sand grout and comparisons will be made with conventional high solids bentonite grouts installed at the same sites.

The long-term performance of GHPs depends on the reliability of the ground heat exchangers and, consequently, the quality of grouting, dimensional stability and bonding characteristics are very critical. It is therefore desirable to evaluate their in-situ conditions. As part of this year's effort, the feasibility of using non-destructive methods for verifying the bond integrity and completeness of grouting in boreholes was investigated. The general approach followed in acoustic methods and the lessons learned from field experience for evaluation of oil wells by the petroleum industry were reviewed. Sonic and ultrasonic methods were compared and the applicability of Cement Bond Logging, Cement Evaluation and Pulse Echo Tools in field verification of GHP ground heat exchangers were investigated. A variety of other non-destructive tests were also considered with emphasis placed on low level vibration techniques.

Finally, a set of engineering evaluations was identified as necessary for validational purposes and to support laboratory and field tests. Two categories of analysis were considered: heat transfer and dynamic response to wave propagation. A two-dimensional finite element model of the ground heat exchanger was developed. Preliminary results from ongoing analysis are presented.

ACKNOWLEDGEMENTS

Firstly, special thanks are due to Lew Pratsch of the U.S. Department of Energy/Office of Geothermal Technologies for continued support of this work. The efforts and hard work of the project collaborators are much appreciated. This includes Professor Steve Kavanaugh at the University of Alabama and the group of students who conducted thermal resistance tests, Dr. Marvin Smith and Randy Perry at Oklahoma State University, and Pat Gronewald, Elton Wright, John Gabaldon and Jim Westmoreland at Sandia National Laboratories. Also, Joe Dobry of Baroid gave valuable assistance at the Sandia field trial. Sincere thanks also to Dr. Ufuk Senturk and Professor Chris Berndt (State University of New York at Stony Brook) for performing the elastic modulus, Poisson's ratio and flexural strength tests. Finally, the interest and encouragement from Harry Roth of the New Jersey Heat Pump Council and Dr. Harvey Sachs of the Geothermal Heat Pump Consortium were of great benefit.

1.0 INTRODUCTION

Geothermal (ground coupled, ground source, GeoExchange) heat pumps (GHPs) are highly efficient systems for heating and cooling residential and commercial buildings. A borehole, typically 4 to 6 in. (102 to 152 mm) diameter and 200 to 300 ft (60 to 90 m) deep, is drilled into the ground. Depending on the system size multiple boreholes may be required. A high density polyethylene (HDPE) U-loop through which water or antifreeze is circulated, is placed in the borehole and connected to the heat pump. The borehole is backfilled with pumpable grout. The grout provides a heat transfer medium between the heat exchanger and surrounding formation, controls groundwater movement and prevents contamination of water supply. The ground is used as either a heat source or heat sink. The required bore length and, hence, installation cost are strongly dependent on the thermal conductivity of the grout.

In addition to thermal conductivity requirements, the grout must be comprised of readily available, environmentally safe and inexpensive components, and must be easy to mix and pump with conventional geotechnical grouting equipment. Furthermore, the grout should have low shrinkage, good bonding characteristics to U-loop and surrounding ground, low permeability and long term durability.

It is common to use granular bentonite-water mixes as grouting materials for GHPs (Eckhart, 1991). However, these grouts have relatively low thermal conductivity that typically ranges from 0.65 to 0.90 W/m.K (Remund and Lund, 1993). The thermal conductivity of bentonite grouts can be improved through incorporation of filler materials such as quartzite sand (Remund and Lund, 1993). A potential drawback of bentonite grouts is loss of thermal conductivity under drying conditions. Also, in some states environmental regulations do not permit the use of bentonite.

Properly designed and mixed cementitious grouts have potential for use as GHP grouts provided that thermal conductivity, cost, durability and other requirements can be met. Brookhaven's research focuses on characterization and optimization of cementitious grouts through use of appropriate mix design and additives. The Brookhaven grout basically consists of Portland cement, a certain grade of silica sand, water, superplasticizer and a small quantity of bentonite.

In FY 97 cement-sand grouts were investigated for thermal conductivity and a range of other properties. The roles of variables such as sand gradation, sand/cement ratio, water/cement ratio, supplementary cementing materials and superplasticizer dosage were examined. The compatibility of optimizing thermal conductivity with other property criteria was studied. The cement-sand grouts were tested for rheological characteristics, bleeding, permeability, bond to HDPE pipe, shrinkage, coefficient of thermal expansion, exotherm, durability and environmental impact. The University of Alabama performed cost analysis and calculations of the reduction in heat exchanger length that could be achieved with such grouts. The results of the FY 97 research are available in the annual report (Allan, 1997).

The grout mix proportions were altered in FY 98 to simplify mixing. The new formulation was characterized for relevant properties. In particular, extensive permeability testing was performed. Two field demonstrations were conducted.

The feasibility of non-destructive testing to evaluate the in-situ condition of ground heat exchangers was investigated. This would be useful for quality control and assurance that the grout is acting as an effective sealant to prevent aquifer contamination. A two-dimensional finite element model of the ground heat exchanger was developed and heat transfer analysis was initiated. The model will also be used in future research to analyze the response of grouted boreholes to different non-destructive methods. Mechanical and physical properties of the grout required for input in future engineering analysis were determined.

2.0 EXPERIMENTAL PROCEDURE

2.1 Materials and Mix Proportions

The basic grout mix consisted of cement, silica sand, water and superplasticizer. Type I cement (ASTM C 150) was used in most of the grout formulations. For one of the boreholes in the field trials Type V (sulfate resistant) cement was used to take potential advantage of the lower heat of hydration. Ground granulated blast furnace slag (BFS) were used as partial replacement for Type I cement in some of the grout formulations.

The superplasticizer (SP) used was a sulfonated naphthalene type with a solids content of 42% by mass and was produced by Master Builders Technologies (Rheobuild 1000). This chemical admixture functions as a dispersant and increases grout fluidity. Thus, superplasticizer allowed the water content of the grout to be reduced while maintaining pumpability. The aim was to keep the water/cementitious material ratio (w/c) as low as possible in order to improve thermal properties, reduce permeability, and increase durability.

Silica sand conforming to the gradation for fine aggregate given by ACI Committee 304 (1991) was used on the basis of previous results (Allan, 1997). This sand was obtained from New Jersey Pulverizing Co. The sieve analysis for the sand is presented in Table 1, along with the specification.

A small proportion of Wyoming bentonite (sodium montmorillonite) was added to some of the cementitious grouts to reduce bleeding, promote full-volume set, and improve sand carrying capacity (i.e., reduce settling). The dosage of bentonite was 2 to 4% by mass of water. Bentonite was used in one of the field trials.

The use of an air entraining agent to improve freeze-thaw durability was investigated. A vinsol resin additive (MB-VR, Master Builders Technologies) that is commonly used in concrete was selected. The air entraining agent was added at a rate of 1 ml/kg cement.

Latex was added to some grout formulations in an attempt to improve bonding to HDPE pipe. The latex used was styrene butadiene copolymer (Tylac 68014-00, Reichold Chemicals) with a polymer solids content of 42%. The polymer solids/cement ratio (p/c) was varied from 0.05 to 0.15. Latex has a tendency to foam and this must be controlled through appropriate mixing procedure and use of an effective antifoam. The Tylac latex already contained silicone antifoam. However, it was found that additional antifoam was required. The antifoam used was D-Air2 (Halliburton).

Recently, a new shrinkage reducing admixture for use in concrete became available. This admixture decreases drying shrinkage by altering surface tension of water and is marketed as Eclipse by W.R. Grace. The dosage rate used was 2% by mass of cement. The amount of water in the grout mix was decreased by a volume corresponding to that of the Eclipse admixture. Since the admixture

increased grout fluidity it was possible to decrease the superplasticizer dosage. The use of lime (CaO) as an expansive agent was also investigated. Lime was at a rate of 6% by mass of cement to selected grout mixes. The BNL grout was also compared with a commercially available expansive grout that contains sand (Conbextra S, Fosroc). The Conbextra S was mixed with a water to solids ratio of 0.209 and this gave a very fluid grout.

Table 1. Specification and Sieve Analysis of Sand Used

Sieve No. (Size, μm)	Percentage Passing (%)	
	ACI 304, Grading 1	Sand Used
8 (3350)	100	100
16 (1180)	95-100	98.84
30 (595)	55-80	66.83
50 (297)	30-55	52.39
100 (149)	10-30	10.75
200 (75)	0-10	0.62

In order to simplify field mixing of the cement-sand grouts, revisions to the mix proportions used in FY 97 were made. Previously, the most promising grouts had a sand to cement ratio (s/c) of 2.5 (by mass). Since the sand is supplied in 100 lb. bags and the cement in 94 lb. bags, a s/c of 2.5 would require using 2.35 bags of sand to one bag of cement. Use of partial bags of sand in the field would be inconvenient and increase the variability of the grout. Therefore, it was decided to investigate the properties of grout produced from mixing two bags of sand to one bag of cement. This gave a s/c value of 2.13. It was necessary to alter the water/cement ratio (w/c) and superplasticizer dosage. The mix proportions of the grouts studied in FY 98 are given in Table 2. Included are the grouts that contained latex. For comparison, the proportions of grouts studied previously are presented in Table 3. Further details of the latter grouts are given in the FY 97 Annual Report (Allan, 1997).

Table 2. Mix Proportions of Cement-Sand Grouts Studied in FY 98.

	111	**112**	**111 0.05L**	**111 0.1L**	**111 0.15L**
Cement (kg/m^3)	590	470	580	570	557
Blast Furnace Slag (kg/m^3)	0	118	0	0	0
Water (l/m^3)	324.5	323.4	287.5	251.6	215.8
Sand (kg/m^3)	1257	1252	1235	1214	1187
Bentonite (kg/m^3)	0 - 13	0	0	0	0
Superplasticizer (l/m^3)	8.8	8.8	5.8	5.7	5.6
Latex (kg/m^3)	0	0	60.4	118.6	173.9
Specific Gravity	2.18	2.17	2.17	2.16	2.14

Table 3. Mix Proportions of Cement-Sand Grouts Studied in FY 97.

	108	**109**	**110**
Cement (kg/m^3)	530	315	312
Blast Furnace Slag (kg/m^3)	0	210	0
Fly Ash (kg/m^3)	0	0	208
Water (l/m^3)	318	315	312
Sand (kg/m^3)	1325	1313	1300
Superplasticizer (l/m^3)	5.3	5.25	5.2
Specific Gravity	2.18	2.16	2.14

Table 4 shows the mix proportions for the neat cement grouts (i.e., no sand) that were studied for comparison. The grouts are designated by their water/cement ratios (w/c).

Table 4. Mix Proportions of Neat Cement Grouts

	47 (w/c = 0.4)	**w/c = 0.6**	**w/c = 0.8**
Cement (kg/m^3)	1369	1087	894
Water (l/m^3)	547.6	652.2	715.2
Superplasticizer (l/m^3)	27.4	0	0
Specific Gravity	1.95	1.74	1.61

The yield and proportions for a batch of Mix 111 grout based on one bag of cement is given in Table 5. Both metric and non-metric units are presented. Note that the superplasticizer content may require adjustment depending on the mixing equipment used and that addition of bentonite may be necessary to reduce bleeding and settling.

Table 5. Mix Proportions and Yield for Single Batch of Mix 111.

Cement	1 x 94 lb. bag
Water	23.5 litres (6.19 U.S. gallons)
Sand (conforming to spec.)	2 x 100 lb. bags
Superplasticizer	639 ml (1.35 pints) (approximately)
Bentonite (optional)	470 g (approximately)
Yield	72.2 litres (19.1 U.S. gallons)

2.2 Mixing

Depending on quantity, the grouts were either mixed in a Hobart planetary mixer, an air-driven grout paddle mixer or an air-driven colloidal grout mixer. The paddle mixer was a ChemGrout CG-550P model with a 34 gallon mixing tank and equipped with a 5 gpm capacity piston pump. The high shear, colloidal mixer was a ChemGrout CG620 model with a capacity of 60 gallons. The properties of the grout, particularly in the unhardened state, depend on the type of mixer used. Thus, some variation between the properties reported here can be expected if different mixing equipment is used. Figure 1 shows the grout being mixed in a paddle mixer at Brookhaven.

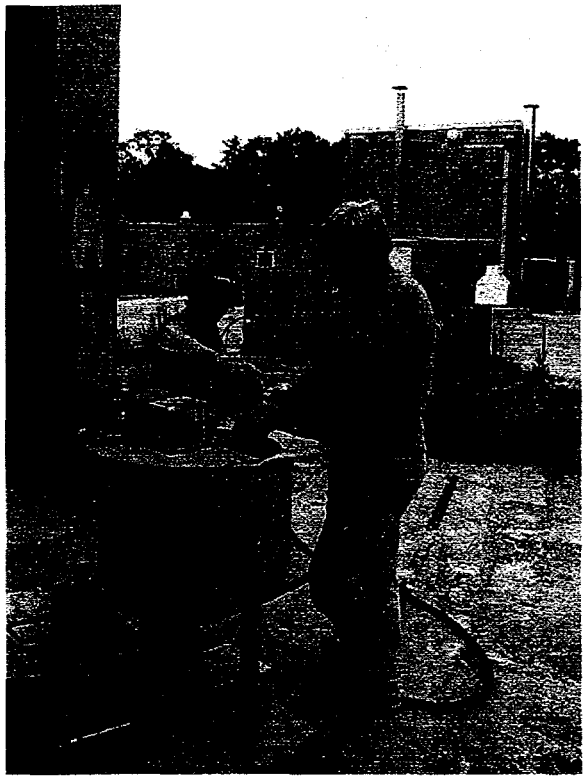

Figure 1. Mixing of grout in paddle mixer at Brookhaven.

2.3 Specific Gravity

The specific gravity of the unhardened grouts was measured following ASTM D 854-83.

2.4 Bleeding

Bleeding of selected grouts was measured following the procedure given in ASTM C 940-89. An 800 ml quantity of freshly mixed grout was poured into 1000 ml glass volumetric cylinder and covered. The heights of grout and any bleed water were monitored up to 4 hours.

2.5 Thermal Conductivity Measurements

The cementitious grouts were cast as blocks 75 mm x 125 mm x 25 mm. Three specimens per batch were cast. The blocks were sealed to prevent evaporation, demoulded after 24 hours and placed in a water bath to cure. The hardened grouts were tested for thermal conductivity at an age of 14 days. The grouts were then dried in an oven at 40°C over a period of seven days, allowed to cool, and re-tested to determine the effect of loss of moisture. In addition, the effect of curing

conditions on thermal conductivity of Mix 111 was determined. Some specimens were placed in a sealed container after demoulding rather than in a water bath.

Thermal conductivity was measured using a Shotherm QTM-D2 Thermal Conductivity Meter. This meter uses the hot wire method to calculate the thermal conductivity, λ. Equation 1 is the basic expression for measurement of λ by this method. The hot wire test is a transient method and therefore overcomes the problem of moisture migration and subsequent decrease in thermal conductivity of moist grouts that would occur with a steady state method. A probe consisting of a heater and thermocouple on the surface of a sole plate with known thermal conductivity is placed on the surface of the material to be tested. Constant current is passed through the heater wire and the electromotive force of the thermocouple at the time is automatically recorded. The thermal conductivity is obtained from Equation 2. Three measurements per specimen were made. Thus, the total number of measurements per grout formulation was nine.

$$\lambda = \frac{q\ln(t_2/t_1)}{4\pi(T_2 - T_1)} \qquad (1)$$

where λ = thermal conductivity (W/m.K)
q = rate of heat flow per unit length (W/m)
t_1 = time 1 (s)
t_2 = time 2 (s)
T_1 = temperature at t_1 (K)
T_2 = temperature at t_2 (K)

$$\lambda = \frac{KI^2 \ln(t_2/t_1)}{V_2 - V_2} - H \qquad (2)$$

where I = current (A)
K and H = constants
V_1 = electromotive force of thermocouple at t_1 (mV)
V_2 = electromotive force of thermocouple at t_2 (mV)

2.6 Permeability

The water permeability (hydraulic conductivity) of the grouts under saturated conditions was measured in a flexible wall triaxial cell permeameter on cylindrical specimens 102 mm diameter and

70 mm long. The permeant was de-aired tap water at room temperature. The applied pressure gradient was 207 kPa (30 psi) over the length of the specimen. The confining pressure applied to seal a latex membrane to the side surface of the grout specimen was 414 kPa (60 psi). The experimental set-up followed that given in ASTM D 5084-90.

Two series of permeability tests were performed. The first series was on bulk grouts. The materials were cast in 204 mm high cardboard cylinders and cut to size after curing using a diamond saw. The second series was on an annulus of grout cast around two axial lengths of 1 in. ID (1.3 in. OD) HDPE Driscopipe® 5300 (Phillips 66). The purpose of this was to represent grout surrounding a U-loop and determine the permeability of the grout/HDPE pipe system. The centre-to-centre separation of the two pipes was 50 mm. These specimens were cast as 204 mm high cylinders and cut to a length of 70 to 80 mm prior to testing in the permeameter. All specimens were insulated for 28 hours after casting so that thermal effects similar to those that may occur in a borehole were simulated. Specimens were demoulded after 24 hours and cured for 28 days in a water bath. An exception to this curing procedure was for latex-modified grouts. These grouts were wet cured for two days and then dried in air. This procedure permits formation of the latex film, where as continuous wet curing does not.

The two embedded pipes were sealed with wax before conducting permeability tests so that water would flow either through the grout or between the grout-pipe interface. This indicated how permeability of the grout-pipe system might be influenced by grout shrinkage and bond quality. A minimum of three specimens per grout mix was tested.

All specimens were vacuum saturated with de-aired water prior to measurement. Volumetric flow rates in and out of the specimens were monitored and measurements commenced when equilibrium was reached. Cement-sand and neat cement grouts were tested.

The effect of temperature on permeability of the grout/pipe specimens was investigated to take into account thermal expansion and contraction of the pipes. The specimens were first tested at room temperature (21°C). Subsequently, the specimens were conditioned in a water bath for 24 hours at 30°C and re-tested. The specimens were then conditioned for 24 hours in water kept in a refrigerator at 1°C and re-tested. Following this, the specimens were subjected to 14 cycles alternating between 30 and 1°C. The duration of each cycle was one day. The final measurement was taken at room temperature. Since the entire specimen was conditioned at the given temperature, the effect of different temperatures in the loop legs as would occur in reality was not replicated. Future work will investigate the effect of actual operating conditions and associated loop leg temperatures on system permeability.

Grout/pipe specimens were also subjected to wet-dry cycles and re-measured for permeability. A batch of specimens was tested after 28 days of wet curing and then underwent 14 wet-dry cycles. These cycles consisted of immersion in water at room temperature for five hours followed by drying in air at room temperature and relative humidity 40-50% for 43 hours.

2.7 Linear Shrinkage

The procedure used to measure linear shrinkage of the grouts is described in ASTM C 490-93a. Grout was cast as beams with dimensions 2 in. x 2 in. x 11.25 in. and the gauge length between embedded studs was 10 in. Four specimens per type of grout were cast. The beams were covered with polyethylene to prevent evaporation and plastic shrinkage cracking. After 24 hours the beams were demoulded and measured for length. Following the initial measurement the beams were stored in polyethylene bags to simulate autogeneous shrinkage. Change in length was measured using a comparator and monitored for up to 92 days.

2.8 Bond Strength

The relative bond strength of selected grouts to HDPE was measured by push out tests. An annulus of grout was cast around an axial length of 1 in. ID (1.3 in. OD) HDPE Driscopipe® 5300 (Phillips 66). The diameter of the specimens was 102 mm and the length was 104 mm. The pipe projected out of the grout by 5 mm. Specimens were insulated after casting for a period of 28 hours. After the initial 28 hour period the grout-pipe specimens were demoulded and placed in a water bath for 28 days. Six specimens per grout batch were tested in a Geotest compression tester. Movement of the pipe was monitored with a dial gauge and LVDT. The load required to push the pipe out 0.04 in. (1 mm) was recorded. Bond strength was calculated as the load divided by the surface area of the embedded pipe.

The effect of temperature on bond strength was investigated by conditioning specimens in water at temperatures of 1, 21 and 35°C. In addition, the bond strength of specimens containing lime as an expansive agent was compared with the strength for identical grouts without lime.

2.9 Freeze-Thaw Durability

The durability of cement-sand grouts subjected to repeated freeze-thaw cycles was determined. Beams 102 mm wide, 76 mm deep and 406 mm long were cast in accordance with ASTM C 666-90. The beams were cured for 28 days prior to testing. A total of 12 beams were tested. Six of these were plain Mix 111 and three were Mix 111 with the air entraining agent. The remaining three beams consisted of plain Mix 111 with an embedded length of 1 in. ID (1.3 in. OD) HDPE Driscopipe® 5300. The purpose of the latter beams was to determine the effect of freeze-thaw cycles on bond between grout and HDPE pipe. The beams were tested in a Logan freeze-thaw cabinet for a total of 300 cycles. The ultrasonic pulse velocity of the beams before and after freeze-thaw cycles was measured to indicate relative deterioration.

2.10 Compressive Strength

Grouts were cast into wax coated cylinders, 102 mm diameter and 204 mm high, for compressive strength tests. The specimens were demoulded after 24 hours and wet cured for 28 days. After curing, the specimens were capped and tested in accordance with ASTM C 39-86 using a Forney compression tester. Six specimens of Mix 111 were tested.

2.11 Splitting Tensile Strength

Cylindrical specimens, 76 mm diameter and 152 mm high, were cast for splitting tensile strength tests. The specimens were demoulded after 24 hours and wet cured for 28 days. After curing, the specimens were trimmed to a length of 140 mm and tested in accordance with ASTM C 496-90 using a Forney compression tester. Six specimens of Mix 111 were tested.

2.12 Flexural Strength

Beams 300 mm x 50 mm x 50 mm of Mix 111 were cast and used to measure flexural strength in accordance with ASTM C 78-94. The beams were demoulded after 24 hours and wet cured for 56 days. Six beams were tested.

2.13 Ultrasonic Pulse Velocity

The ultrasonic pulse velocity of grout was measured for two purposes. The first of these was for determination of the compression, or P-wave velocity for use in modelling the response of grout to wave propagation. Six cylinders of Mix 111 grout were cast and wet cured for 28 days. The cylinders were 76 mm diameter and initially 152 mm long. After curing the ends of the cylinders were trimmed with a cut-off saw to give even surfaces. Ultrasonic pulse velocity was measured following the procedure given in ASTM 597-83. A Pundit meter with a 54 kHz transmitting transducer was used. The effect of drying on P-wave velocity was determined by allowing the grout cylinders to dry in air and re-measuring the velocity. Changes in specimen density were also monitored so that the acoustic impedance could be calculated. This is the product of P-wave velocity and density.

The second use of ultrasonic pulse velocity testing was to non-destructively monitor degradation associated with freeze-thaw cycles. In this case the P-wave velocity of grout beams before and after freeze-thaw tests was measured.

2.14 Elastic Modulus and Poisson's Ratio

The elastic modulus and Poisson's ratio of Mix 111 was measured following ASTM C 469. A compressometer/extensometer arrangement as described in the standard was employed. Figure 2 depicts the experimental equipment. This test determines the static modulus under compression.

The elastic modulus was required for the modelling activity. It would also be worthwhile to measure the dynamic modulus in the future since this is typically not equivalent to the static modulus for cementitious materials. A batch of 17 grout cylinders, 102 mm in diameter and 204 mm long, were cast. The cylinders were wet cured for 28 days and then capped. Six of the cylinders were used for compressive strength tests as described above. The remaining cylinders were used for elastic modulus and Poisson's ratio tests. The cylinders were tested in a hydraulic Instron testing machine. The ultimate capacity of this machine was 100 kN. The test procedure called for measuring the longitudinal and transverse strains at a load equivalent to 40% of the ultimate load. Based on the average ultimate load determined from the compressive strength tests, 40% of the ultimate load equated to 120 kN. Therefore, it was decided to measure strains at 30% of the ultimate load so that the capacity of the testing machine would not be exceeded. This was in the elastic range of the stress-strain curve. Each specimen was loaded three times. Measurements taken after the initial loading were used to calculate elastic modulus and Poisson's ratio.

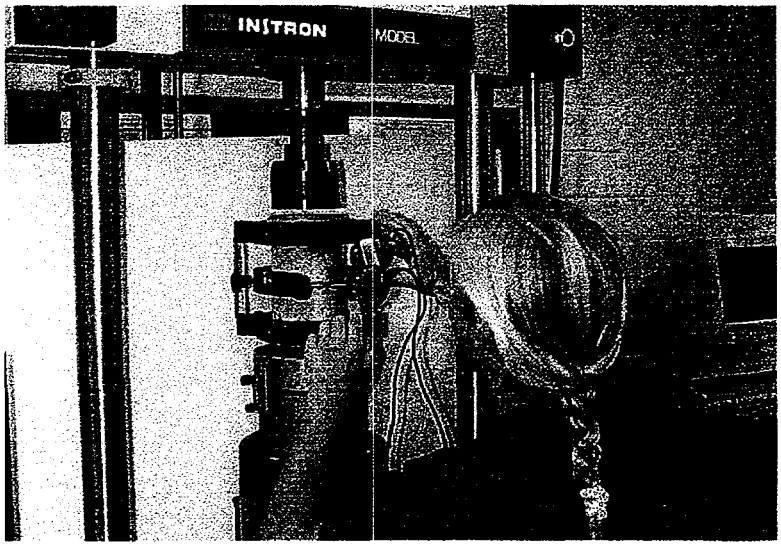

Figure 2. Compressometer/extensometer arrangement for elastic modulus and Poisson's ratio tests.

2.16 Thermal Resistance Tests

A team of senior mechanical engineering students (Fred Aragon, Johnny Belmont, Homer Parton and Ross Strickland) under the direction of Professor S. Kavanaugh at the University of Alabama conducted thermal resistance tests on Mixes 111 and 112. This was a continuation of previous tests performed last year and full results are described in the report by Aragon et al., (1998). A rig has been constructed at the University of Alabama to enable measurement of net thermal resistance per unit length of a 10 ft long tube that contains a single U-loop backfilled with grout. The rig can accommodate either 4 inch or 6 inch diameter tubes. The grouted tube is placed inside an

8 inch diameter PVC pipe jacket. Cold well water is circulated in the jacket. Temperatures are monitored by numerous thermocouples, along with flow rate and power to the water heater. This year's student team modified the rig to enable tests that simulated operation of a heat pump in heating mode. Such tests can determine the effect of thermal contraction of the U-loop on the heat transfer behaviour.

Two 4 inch diameter tubes and one 6 inch diameter tube were grouted and delivered to the University of Alabama for testing. The 4 inch tubes were filled with two slightly different variations of Mix 111. The difference was the superplasticizer dosage and that affects the grout pumpability and shrinkage. One tube had a superplasticizer dosage of 12 ml/kg cement while the other tube had 15 ml/kg cement. The 6 inch tube was filled with Mix 112 (slag modified) but was not tested due to time constraints. It was observed during the mixing of the Mix 111 grouts that some air entrainment occurred. The cause of this was later identified to be the use of cement that contained a waterproofing additive. The additive was probably some type of stearate and this resulted in excessive air content. Therefore, it is important that cement used with this type of grout does not contain such an additive.

3.0 EXPERIMENTAL RESULTS

3.1 Bleeding

The results of the bleed tests on Mix 111 with different superplasticizer and bentonite contents are presented in Table 6. (Bentonite/water content is noted as b/w). These mixes were prepared in a Hobart mixer. Different results may be obtained with other mixers.

Table 6. Bleed Test Results

Time (hr)	% Bleed				
	111 (w/c = 0.55; 12 ml SP/kg cement)	**111(w/c = 0.54; 15 ml SP/kg cement)**	**111 (w/c = 0.55; 15 ml SP/kg cement)**	**111 (w/c = 0.55; 15 ml SP/kg cement; b/w = 0.02)**	**111 (w/c = 0.55; 15 ml SP/kg cement; b/c = 0.04)**
0.5	0.12	0.06	0.12	0.12	0.0
1	0.25	0.12	0.37	0.12	0.0
1.5	0.25	0.25	0.50	0.12	0.0
2	0.37	0.37	0.62	0.12	0.0
2.5	0.37	0.37	0.62	0.12	0.0
3	0.37	0.37	0.62	0.12	0.0
4	0.37	0.5	0.75	0.12	0.0

3.2 Specific Gravity

The specific gravity of Mix 111 was measured to be 2.18. This is equivalent to 18.2 lb./gallon.

3.3 Thermal Conductivity

The thermal conductivity of Mix 111 in the wet and dry states is presented in Table 7. Also given are the values obtained for the grout formulation containing an air entraining agent (111 AE) and the Conbextra S grout. All of these grouts were wet cured prior to testing. The latex-modified grout was wet cured for two days and then allowed to dry in air for 12 days. The specimens were then vacuum saturated before measuring thermal conductivity. The results of the tests are reported

in Table 8. The thermal conductivity of Mix 111 when cured in a sealed container rather than in water was 2.104 ± 0.049 W/m.K for the first batch and 2.210 ± 0.037 W/m.K for the second.

Thermal conductivity results for neat cement grouts and other cement-sand grout formulations are given in the FY 1997 Annual Report (Allan, 1997).

Table 7. Thermal Conductivity of Wet Cured Grouts. (1 W/m.K = 0.578 Btu/hr.ft.°F).

Grout Mix	Thermal Conductivity, W/m.K	
	14 Days	After Drying
111	2.423 ± 0.045	2.160 ± 0.038
111 AE	1.753 ± 0.029	1.552 ± 0.030
Conbextra S	1.771 ± 0.034	1.613 ± 0.032

Table 8. Thermal Conductivity of Latex-Modified Grout. (1 W/m.K = 0.578 Btu/hr.ft.°F).

Grout Mix	Thermal Conductivity, W/m.K	
	14 Days (saturated)	After Drying
111 0.15L	2.276 ± 0.045	2.196 ± 0.039

3.4 Coefficient of Permeability

The coefficient of permeability (hydraulic conductivity) of bulk Mix 111 is given in Table 9 along with data for previously tested cement-sand and neat cement grouts for comparison. It is noted that the coefficient of permeability of Mix 111 was measured on 102 mm diameter specimens whereas the other cement-sand and neat cement grout specimens were 76 mm diameter. The system permeabilities of grout-pipe specimens at different temperatures are given in Tables 10 and 11. The system permeabilities are also compared graphically in Figure 3. Table 12 shows the results for the Mix 111 grout/pipe specimens subjected to thermal cycles and wet-dry cycles. Neat cement/pipe specimens underwent cracking during thermal and wet-dry cycles and could not be tested. The results for the latex-modified grouts are presented in Table 13.

The grout-pipe specimens that contained Eclipse shrinkage reducing admixture were found to have cracked when demoulded. The same specimens were re-cast and the same problem occurred. Therefore, the use of this admixture was discontinued and no specimens were tested.

Infiltration tests on grouted tubes containing a single U-loop are also in progress and the results will be reported in the future.

Table 9. Bulk Coefficient of Permeability Data for Mix 111 and Previously Tested Cement-Sand Grouts.

Grout Mix	Permeability (cm/s)
Mix 111	$1.58 \times 10^{-10} \pm 5.2 \times 10^{-11}$
Mix 108	$5.1 \times 10^{-10} \pm 1 \times 10^{-10}$
Mix 109	$4.9 \times 10^{-10} \pm 7 \times 10^{-11}$
Mix 110	$5.8 \times 10^{-10} \pm 9 \times 10^{-11}$

Table 10. Coefficient of Permeability of Neat Cement Grout-Pipe Specimens at Different Temperatures.

Grout Mix	Temperature (°C)	Permeability (cm/s)
w/c = 0.4	1	$4.87 \times 10^{-5} \pm 3.1 \times 10^{-6}$
w/c = 0.4	21	$6.30 \times 10^{-6} \pm 2.5 \times 10^{-7}$
w/c = 0.4	30	$2.68 \times 10^{-6} \pm 4.3 \times 10^{-7}$
w/c = 0.6	1	$5.10 \times 10^{-5} \pm 5.6 \times 10^{-6}$
w/c = 0.6	21	$7.48 \times 10^{-6} \pm 9.0 \times 10^{-7}$
w/c = 0.6	30	$2.37 \times 10^{-6} \pm 3.2 \times 10^{-7}$
w/c = 0.8	1	$8.40 \times 10^{-5} \pm 9.8 \times 10^{-6}$
w/c = 0.8	21	$1.06 \times 10^{-5} \pm 1.2 \times 10^{-6}$
w/c = 0.8	30	$5.87 \times 10^{-6} \pm 6.3 \times 10^{-7}$

Table 11. Coefficient of Permeability of Mix 111 and Conbextra S Grout-Pipe Specimens at Different Temperatures.

Grout Mix	Temperature (°C)	Permeability (cm/s)
111	1	$1.57 \times 10^{-5} \pm 2.5 \times 10^{-6}$
111 (Batch 1)	21	$1.93 \times 10^{-7} \pm 2.1 \times 10^{-8}$
111 (Batch 2)	21	$2.76 \times 10^{-7} \pm 3.4 \times 10^{-8}$
111	30	$1.58 \times 10^{-7} \pm 2.0 \times 10^{-8}$
111	35	$5.37 \times 10^{-8} \pm 4.7 \times 10^{-9}$
Conbextra S	21	$2.89 \times 10^{-6} \pm 4.1 \times 10^{-7}$

Table 12. Coefficient of Permeability of Mix 111 Grout-Pipe Specimens Subjected to Thermal Cycles and Wet-Dry Cycles.

Wet-Dry Cycles		Thermal Cycles	
Initial Permeability (cm/s)	**Final Permeability (cm/s)**	**Initial Permeability (cm/s)**	**Final Permeability (cm/s)**
$2.76 \times 10^{-7} \pm 3.4 \times 10^{-8}$	$4.44 \times 10^{-7} \pm 3.9 \times 10^{-8}$	$1.93 \times 10^{-7} \pm 2.1 \times 10^{-8}$	$3.41 \times 10^{-7} \pm 3.9 \times 10^{-8}$

Table 13. Coefficient of Permeability of Latex-Modified Grout-Pipe Specimens at Different Temperatures.

Grout Mix	Temperature (°C)	Permeability (cm/s)
111 0.05L	21	$6.37 \times 10^{-7} \pm 8.2 \times 10^{-8}$
111 0.1L	21	$5.84 \times 10^{-7} \pm 7.8 \times 10^{-8}$
111 0.15L	1	$4.03 \times 10^{-5} \pm 5.9 \times 10^{-6}$
111 0.15L	21	$2.80 \times 10^{-7} \pm 4.5 \times 10^{-8}$
111 0.15L	30	$1.22 \times 10^{-7} \pm 3.6 \times 10^{-6}$

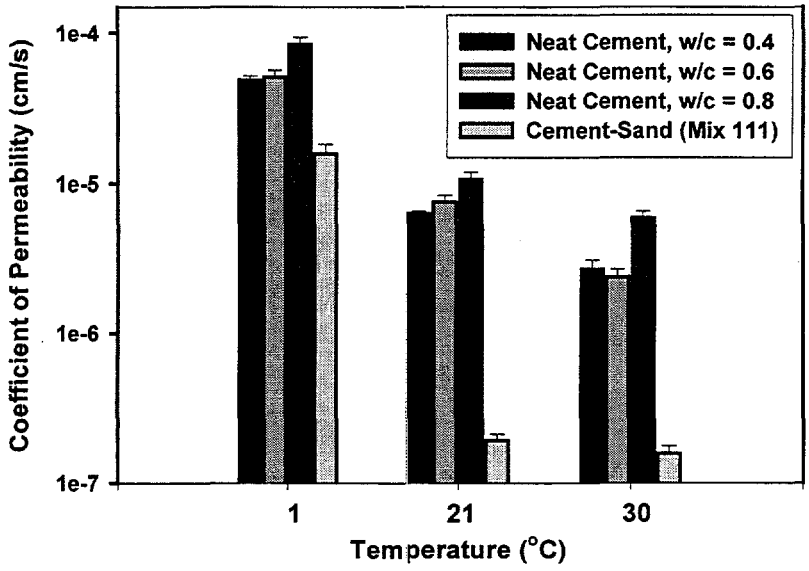

Figure 3. Coefficient of permeability of grout-pipe specimens at different temperatures.

3.5 Linear Shrinkage

The results of the linear shrinkage tests on Mix 111 are averaged in Figure 4.

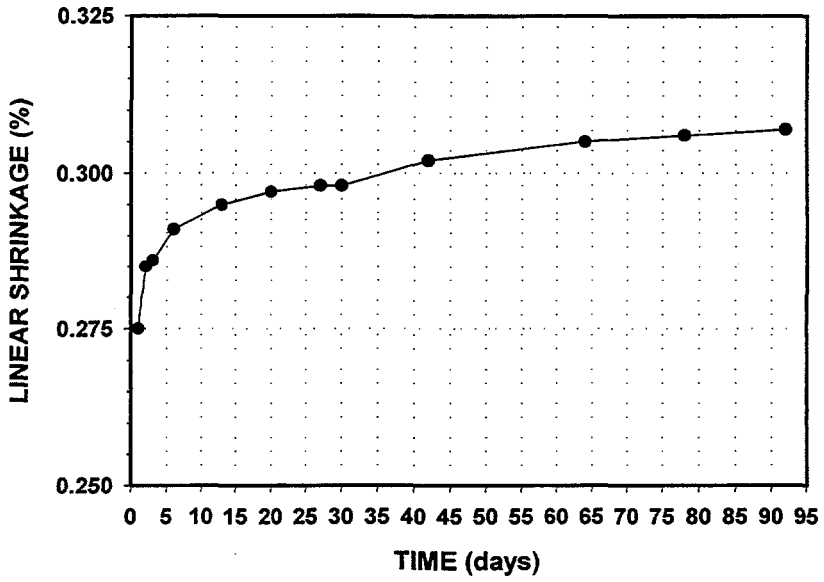

Figure 4. Linear Shrinkage versus Time for Mix 111.

3.6 Bond Strength

The results of the bond strength tests conducted at room temperature are presented in Table 14 and Figure 5. The average and standard deviation for six specimens are given. Also included are previous results for other cement-sand and neat cement grouts. Table 15 and Figure 6 show the effect of temperature on bond strength for Mix 111.

Table 14. Bond Strength Results

Grout Mix	Bond Strength (kPa)
47 (w/c = 0.4)	3.6 ± 0.7
108	72.4 ± 12.9
109	73.0 ± 10.3
110	47.0 ± 10.8
111	150 ± 20.5
111 + CaO	69.5 ± 13.4

Table 15. Effect of Temperature on Bond Strength for Mix 111.

Temperature (°C)	Bond Strength (kPa)
1	20.0 ± 1.4
21	150 ± 20.5
35	329 ± 39.0

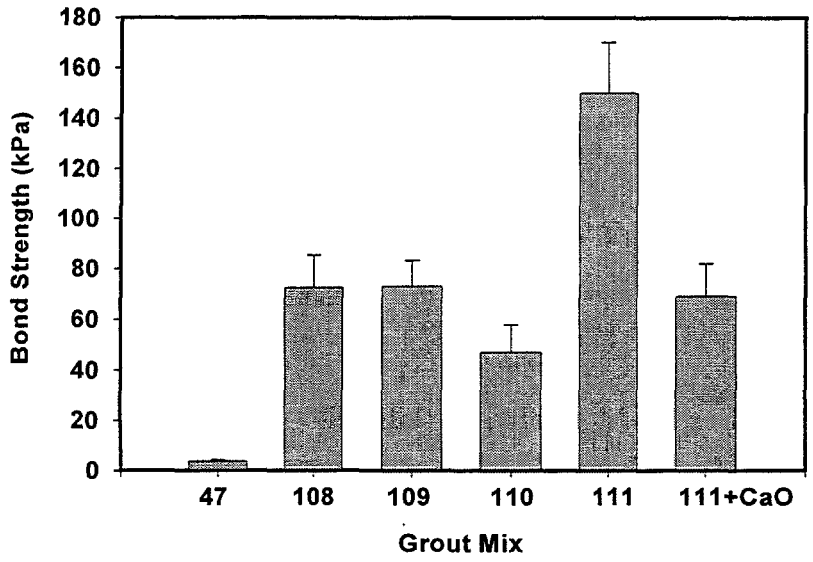

Figure 5. Bond Strengths for Different Grout Mixes.

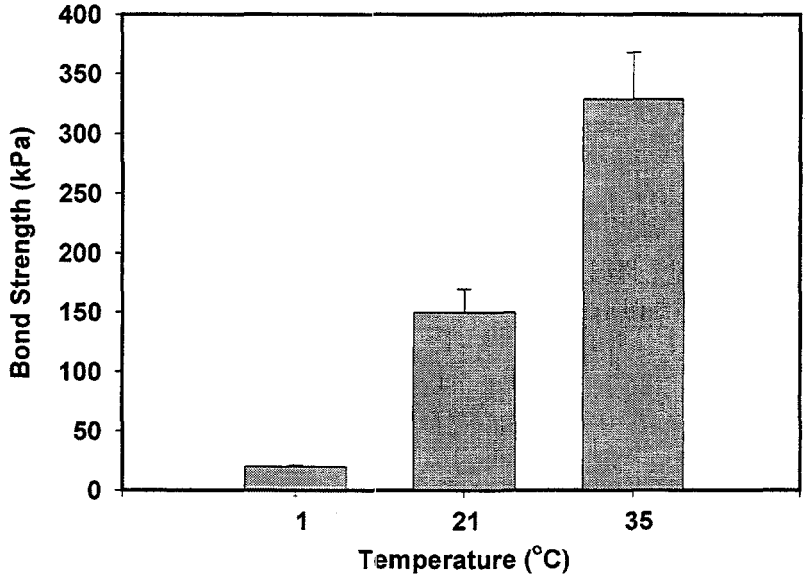

Figure 6. Bond Strength of Grout Mix 111 versus Temperature.

3.7 Microstructure

Specimens used in the permeability tests were sectioned and viewed under an optical microscope to examine the integrity of the bond to HDPE. Neat cement grout (Mix 47, w/c = 0.4) was observed to have gaps between the pipe and grout which were 0.05 to 0.325 mm wide. The interfacial gaps present for Mix 111 were 0.025 to 0.075 mm wide. Gaps less than 0.01 mm wide were observed for the latex-modified grouts. Although the bond integrity appeared visibly improved by addition of latex, the permeability tests indicated that sealing ability of the grout was not enhanced and that the unmodified grout had superior impermeability. It is possible that the small gaps observed for the latex-modified grout were an anomaly and not representative of the typical interfacial structure.

3.8 Freeze-Thaw Durability

After 300 freeze-thaw cycles Mix 111 exhibited slight surface scaling. The grout containing an air entraining agent had improved freeze-thaw resistance and only very slight surface damage occurred. However, air entrainment led to a decrease in thermal conductivity as shown in Table 7. The beams containing a length of HDPE pipe were sectioned and examined under an optimal microscope. It was found that the bond was not significantly affected in that the gap between pipe

and grout was similar to that for specimens not subjected to freeze-thaw cycles. The changes in ultrasonic pulse velocity after the freeze-thaw tests are given in Table 16.

Table 16. Ultrasonic (P-Wave) Velocity Before and After Freeze-Thaw Cycles.

Grout Mix	Ultrasonic Pulse Velocity (km/s)		% Change
	Initial	Final	
111	4.17 ± 0.10	3.86 ± 0.17	-7.4
111 AE	3.91 ± 0.00	3.91 ± 0.00	0.0

3.9 Mechanical Properties

The mechanical properties of Mix 111 are summarized in Table 17.

Table 17. Mechanical Properties of Mix 111.

Compressive Strength (MPa)	36.7 ± 4.2
Flexural Strength (MPa)	6.35 ± 0.72
Splitting Tensile Strength (MPa)	6.01 ± 0.48
Elastic Modulus (GPa)	13.8 ± 0.9
Poisson's Ratio	0.21 ± 0.02

3.10 Ultrasonic Pulse Velocity

The effect of drying in air at room temperature on ultrasonic pulse (P-wave) velocity for Mix 111 is shown in Figure 7. The change in acoustic impedance with drying is depicted in Figure 8. Attempts were made to measure the P-wave velocity of thermally enhanced bentonite and high solids bentonite for comparison. However, the transit times exceeded the range of the Pundit meter and velocity could not be determined. Furthermore, both types of bentonite grouts underwent cracking after one day of drying in air, with the high solids bentonite being worse.

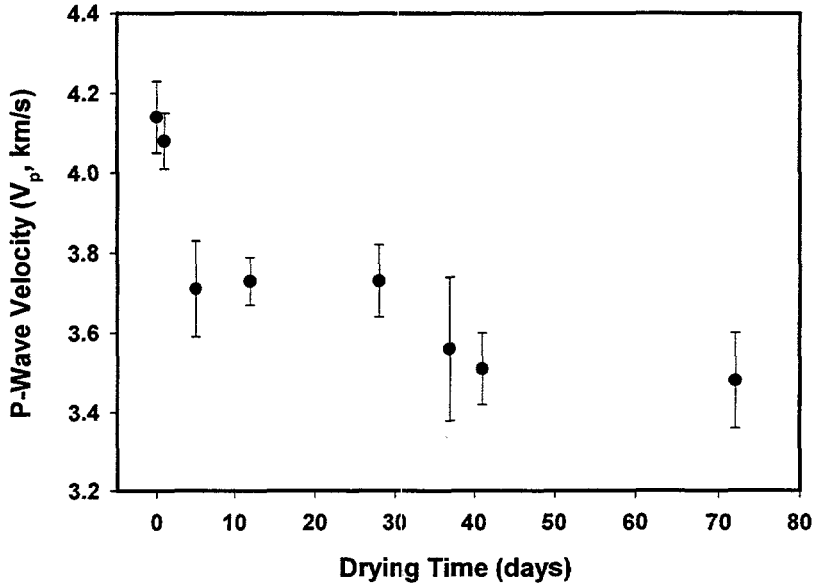

Figure 7. P-Wave Velocity of Mix 111 versus Drying Time.

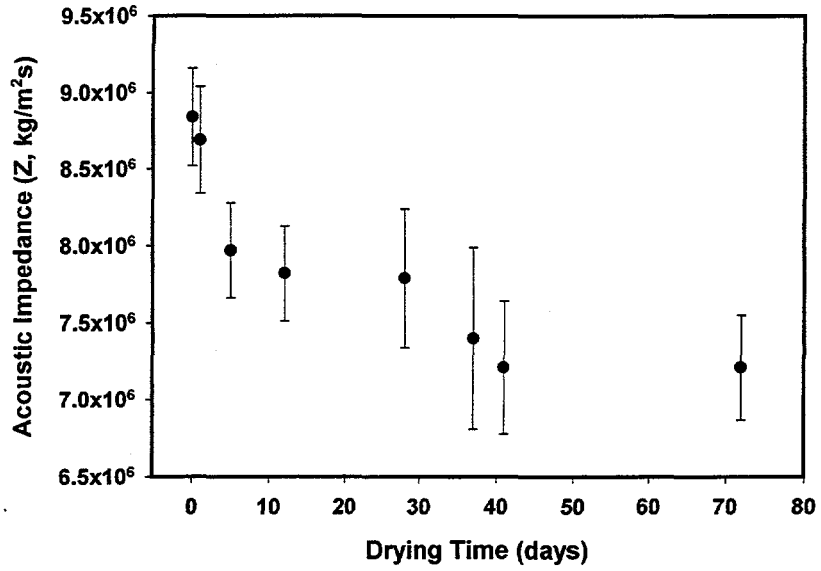

Figure 8. Acoustic Impedance of Mix 111 versus Drying Time.

3.11 Thermal Resistance

Different grouts were mixed with either a paddle of colloidal mixer and pumped into tubes containing a single U-loop. The grouted tubes were then shipped to the University of Alabama for testing. The complete results are described in the report by Aragon et al. (1998). The results are also to be presented at next year's ASHRAE conference (Kavanaugh and Allan, in press). The thermal resistance tests performed last year were reported by Peek et al. (1997).

Thermal resistance tests on grout Mix 111 with different superplasticizer dosage were performed in both heating and cooling mode. The heating mode test was of particular interest since the effect of thermal contraction of the U-loop could be investigated. The calculated and experimental thermal resistances were compared. The overall theoretical thermal resistance, $R_{overall}$ was calculated as follows:

$$R_{grout} = 1/\lambda_{grout} S_b \quad where\ S_b = 17.44\left(\frac{D_{Bore}}{D_o}\right)^{-0.6052} \tag{3}$$

$$R_{pipe} = \left(\frac{\ln D_o / D_i}{2\pi\lambda_p} + \frac{1}{\pi D_i h_i} \right) \div 2 \quad (4)$$

$$R_{overall/calc} = R_{grout} + R_{pipe}. \quad (5)$$

where D_{Bore} = diameter of borehole (ft)
D_i = inside diameter of U-loop (ft)
D_o = outside diameter of U-loop (ft)
h_i = internal heat transfer coefficient (Btu/hr.ft^2.°F)
λ_{Grout} = thermal conductivity of grout (Btu/hr.ft.°F)
λ_p = thermal conductivity of pipe (Btu/hr.ft.°F)

The experimental overall thermal resistance was determined by:

$$R_{overal\ /\exp} = \frac{t_{Avg\ .U-loop} - t_{Avg\ .Steel\ Tube}}{q} \quad (6)$$

The average temperature, $t_{Avg.U\text{-}loop}$, for the U-loop was the average of the inlet and outlet values while the steel tube temperature, $t_{Avg.Steel\ tube}$, was the average of the six values measured at different locations along the length of the tube. The heat rate, q, was calculated by Equation 7:

$$q = \rho\ Q\ c_p\ (t_{wo} - t_{wi}) \quad (7)$$

where ρ = density of water
Q = volumetric flow rate of water
c_p = specific heat
t_{wo} = outlet water temperature
t_{wi} = inlet water temperature

The calculated and experimental overall thermal resistances are presented in Table 18.

Table 18. Calculated and experimental overall thermal resistance for Mix 111.

Grout Mix	Cooling Mode		Heating Mode	
	R_{exp} (hr.ft.°F/Btu)	R_{calc} (hr.ft.°F/Btu)	R_{exp} (hr.ft.°F/Btu)	R_{calc} (hr.ft.°F/Btu)
111 (SP = 15 ml/kg cement)	0.143	0.157	0.158	0.164
111 (SP = 12 ml/kg cement)	0.151	0.157	0.140	0.164

4.0 DISCUSSION OF EXPERIMENTAL RESULTS

4.1 Bleeding

The results show that bleeding increases as w/c and superplasticizer dosage increase. A small amount of bleeding is probably not of great concern for the GHP application. However, excessive settling of sand is detrimental to the grout uniformity and stability. The type of grout mixer used will also influence the grout stability and tendency to bleed. Bleeding tends to be more pronounced in low shear mixers (e.g., paddle mixers). Addition of bentonite decreased bleeding and the degree of sand settlement. However, bentonite also increases grout viscosity. A possible alternative to using bentonite to control bleeding would be a suitable water-soluble polymer such as welan gum (Skaggs et al., 1994; Khayat and Yahia, 1997). The latex-modified grouts did not exhibit any bleeding.

Bleeding and segregation were found to be problems during the first field trial at Oklahoma State University and this was corrected by the second trial at Sandia National Laboratories. The field trials are discussed further in Section 5.0.

4.2 Thermal Conductivity

Mix 111 has a relatively high thermal conductivity in the moist and dry states. The value of 2.423 W/m.K compares with 0.803 to 0.868 W/m.K for neat cement grouts tested last year (Allan, 1997), 0.75 to 0.80 W/m.K for conventional high solids bentonite and 1.46 W/m.K for thermally enhanced bentonite. The thermal conductivity of Mix 111 is slightly lower than the cement-sand grouts tested previously which had a sand/cement ratio of 2.5. Retention of thermally conductive properties under dry conditions is an important requirement. The thermal conductivity of Mix 111 decreased 11% on drying. The decrease in conductivity is reversible on re-saturation.

Curing conditions also affected thermal conductivity. Mean values for two different batches were 2.104 and 2.210 W/m.K when Mix 111 was cured under sealed conditions rather than wet. The thermal conductivity was similar to that for the oven dried grout. It can be expected that the thermal conductivity of grouts used to backfill boreholes will depend on the curing conditions and moisture content.

Addition of an air entraining agent to Mix 111 resulted in a significant decrease in thermal conductivity due to the formation of a network of air bubbles. Any other cause of air bubbles in the hardened grout will decrease conductivity. For example, it was found that cements that already contained a waterproofing agent tended to foam. The Conbextra S grout had a lower thermal conductivity than Mix 111. This was attributed to the lower sand content.

The vacuum saturated latex-modified grout had slightly lower thermal conductivity than the equivalent mix without latex. Therefore, latex is not detrimental to grout conductivity for the mix proportions and conditions tested.

4.3 Permeability

The permeability of bulk Mix 111 was relatively low. Reduction of w/c from 0.6 for Mixes 108, 109 and 110 to 0.55 for Mix 111 improved the impermeability. While permeability of the bulk material is an important property, the permeability of the grouted borehole system is of key interest for evaluating the ability of the grout to act as an effective sealant. Since the bonding between grout and U-loop is imperfect the permeability of the grout/loop system is not equivalent to that of the bulk grout. This principle is applicable to all grout types, not just cementitious. In last year's research the permeabilities of 3 inch diameter grout specimens with an axially embedded length of HDPE were measured. This year the permeameter was modified to accommodate 4 inch diameter specimens containing two lengths of pipe. This configuration was a more realistic simulation of a grouted borehole.

It was determined that the grout/pipe permeabilities were higher than that of bulk grout and that the permeability depended on grout mix proportions and test temperature. This is attributed to a higher permeability pathway at the grout/pipe interface, which was confirmed by microstructure studies. The change in permeability with temperature is due to thermal expansion and contraction of the HDPE pipe. The results in Tables 10 and 11and Figure 3 indicate the relative performance of neat cement grouts with different values of w/c and Mix 111. At room temperature the mean permeability of Mix 111/pipe specimens was 1.93×10^{-7} cm/s compared with 6.30×10^{-6} to 1.06×10^{-5} cm/s for neat cement grouts. When the specimens were conditioned at 30°C the improvement in impermeability between the neat cement grouts and Mix 111 was an order of magnitude. At 35°C Mix 111 showed a further reduction of permeability to 5.37×10^{-8} cm/s. The grout/pipe permeabilities increased significantly to the magnitude of 10^{-5} cm/s for specimens conditioned at 1°C. The performance of Mix 111 remained better than that for the neat cement grouts, although the difference was not as great at the lower temperature. While the bonding to HDPE pipe is not perfect, the ability of the cement-sand grout to act as a sealant is better than that of neat cement.

For the neat cement grout/pipe specimens it was found that permeability tended to increase with increasing w/c as expected. The permeability of the Conbextra S grout/pipe specimens was relatively high and corresponded with visible interfacial gaps.

The results can be compared with other systems, which involve bonding between grout and another material. Kurt and Johnson (1982) and Edil et al. (1992) have investigated the permeability of grout/casing systems for sealing boreholes. Kurt and Johnson (1982) found that increasing w/c of neat cement grout from 0.46 to 2.0 increased the grout/PVC casing system permeability significantly. Permeability varied with test pressure and ranged from 2 to 10×10^{-4} cm/s for w/c = 0.46 and 2.6 to 7.7×10^{-3} cm/s for w/c = 2.0. In the study by Edil et al. (1992), infiltration tests were

performed on the annulus of different grouts around metal casing. Neat cement grouts were found to allow infiltration at the grout/casing interface for a limited distance. Bentonite grouts exhibited varying performance. Benseal® was found to have good sealing characteristics compared with Volclay® and Quik-Gel®.

When reviewing the grout/pipe permeability results at different temperatures the fact that the entire specimen was conditioned at a given temperature must be considered. Hence, the effect of different temperatures in the loop legs as would occur during operation of a GHP was not reproduced. The tests performed to date have not included the bond between grout and surrounding formation. Therefore, some differences between the results reported here and the permeability of a grouted borehole in service can be expected.

The performance of the latex-modified grouts (Table 13) was not as good as those without latex. Despite the apparent reduction in interfacial gaps as viewed under a microscope, the permeability was not improved by addition of latex. As mentioned previously, the good interfacial bonding characteristics observed may have been a specimen anomaly and not indicative of the typical microstructure. Since latex is relatively expensive and there does not appear to be a benefit with respect to permeability, use of latex seems unwarranted at this stage.

It was observed that the coefficient of variation of permeability for the grout/pipe specimens was higher than that bulk material. Also, the permeabilities of specimens cut from the same original cylinder were often very different. Therefore, the interfacial variability contributes to the variability in permeability. For all of the grout/pipe specimens it is possible that there was leakage between the wax used to seal the pipes and the pipe walls. This may create some errors in the permeability data.

Thermal cycling was found to cause an increase in Mix 111 grout/pipe permeability by a factor of 1.7. Similarly, wet-dry cycles increased system permeability by a factor of 1.6. Both tests were an aggressive simulation of conditions to which the grout would be subjected in service since the cycle time was short. The neat cement grouts exhibited radial cracking when dried in air or when placed in the water bath at 30°C. Also, some of the neat cement grouts with w/c = 0.6 cracked when molten wax was poured into the pipes to seal them during the specimen preparation phase. The tendency for cracking of the neat cement grouts on radial expansion of the HDPE pipe is associated with the material's low tensile strength and fracture toughness. Hence, the Mix 111 grout shows resistance to this form of failure.

In-situ permeability or infiltration tests on grouted boreholes would be valuable to confirm the sealing ability of the cement-sand grout under real life operating conditions. Such tests could also be performed on other types of grout for comparison.

4.4 Linear Shrinkage

Figure 4 illustrates the average linear shrinkage versus time of Mix 111 stored in plastic bags. The initial shrinkage within the first 24 hours was 0.275% and the shrinkage after 92 days was 0.307%. By comparison, the equivalent values for Mix 108 tested last year were 0.202% and 0.263%, respectively. The increased shrinkage of Mix 111 can be attributed to the lower sand content and higher superplasticizer dosage.

The type of shrinkage measured in this test was autogeneous. Autogenous shrinkage is associated with self-desiccation and represents shrinkage when there is no moisture loss or gain. Other types of shrinkage that may be encountered are plastic and drying. Plastic shrinkage occurs while the grout is still in the unhardened state. Suction of water into surrounding dry soil or rock may occur and contribute to plastic shrinkage. If the surrounding formation is moist as a result of drilling fluids or groundwater when the grout is placed, plastic shrinkage will be reduced. Drying shrinkage of the grout may occur in dry subsurface conditions or when heat is rejected by the heat exchanger into the ground. An increase in moisture content will result in swelling, although initial drying shrinkage is not fully reversible on wetting (Neville, 1996). Volume changes can be expected with seasonal variations and GHP operational mode. The presented data does not include the effects of moisture transients on grout shrinkage/expansion.

The use of Eclipse shrinkage reducing admixture was found to cause cracking of grout/pipe specimens within the first 24 hours. Hence, its use is not recommended without further evaluation. Addition of lime (CaO) as an expansive agent to Mix 111 decreased bond strength as discussed below.

4.5 Bond Strength

The results of the bond strength tests at room temperature in Figure 5 show that cement-sand grouts have superior bonding characteristics to neat cement. This is due to the relatively high shrinkage and expected higher exotherm of neat cement grouts. Mix 111 had the highest bond strength of the different cement-sand grout formulations and this is probably the result of lower water/cement ratio. Despite the higher shrinkage compared with Mix 108, the bond strength of Mix 111 was better. Addition of lime did not improve bond strength of Mix 111. Although lime should act as an expansive agent, the increased exotherm with this additive caused a reduction in bond integrity presumably due to thermal expansion and subsequent contraction of the embedded pipe. The bond strength specimens were wet cured and differences in bond strength may arise from different curing conditions.

Figure 6 shows the effect of temperature on bond strength for Mix 111. It was observed that bond strength is significantly reduced at low temperatures due to contraction of the HDPE pipe. At elevated temperature the bond strength increases as the pipe expands. Therefore, the bonding characteristics are strongly temperature dependent. As was the case for the grout/pipe permeability

tests, the bond strength specimens were conditioned at a given temperature and the effect of different temperatures in the loop legs as would occur in practice was not reproduced. Therefore, some variation in bonding performance between the laboratory specimens and an operating GHP system can be expected.

This work has not yet examined the bond between grout and surrounding formation. Haberfield and Baycan (1997) have studied the bond between rock and grout and the effect of calcium sulphoaluminate as an expansive agent. Bond strength was found to increase with addition of the expansive agent for 98 mm diameter anchors whereas the effect was less pronounced for diameters of 300 mm.

Another possible means of improving grout bond to surrounding ground is pressurized grouting. This procedure is used where grout/ground bond is of prime importance such as in geotechnical applications. An example of this is for micropiles (Bruce et al., 1995). The practicality and economics versus benefits of employing pressurized grouting techniques for GHPs would require further evaluation before any recommendations can be made.

4.6 Freeze-Thaw Durability

Operation of a geothermal heat pump in the heating mode can result in freezing of the media surrounding the heat exchanger. Freezing of grout above the frost line in northern climates is also possible. Freezing of water held within cement paste pores results in dilating pressures and subsequent cracking. Resistance to damage induced by freeze-thaw cycles depends on degree of saturation and pore structure. Saturated cementitious materials are more susceptible to deterioration than dry materials. Freeze-thaw resistance of concrete and other cementitious materials can be improved through the use of air entraining agents. The freeze-thaw tests showed that Mix 111 grout without an air entraining agent underwent slight surface deterioration and that performance was improved by air entrainment. However, air entrainment decreased the thermal conductivity due to production of discontinuous air bubbles. For non-air entrained concrete the freeze-thaw resistance is improved by reducing water/cement ratio (Neville, 1996).

4.7 Mechanical Properties

The Mix 111 had a moderate compressive strength of 36.7 ± 4.2 MPa. This property is probably not of great importance for GHP applications but can serve as a means of quality control since its is controlled by mix proportions. Since it is difficult to perform direct tension tests on cementitious materials, indirect methods were used. These were flexure and splitting tension tests. The flexural strength of Mix 111 was 6.35 ± 0.72 MPa and the splitting tensile strength was 6.01 ± 0.48 MPa. It is noted that the beams for the flexural strength tests were cured for 56 days whereas the cylinders for splitting tensile strength tests were 28 days old. Hence, the impact if different curing times needs to be taken into consideration. For concrete the direct tensile strength is around

¾ the theoretical flexural strength and 5 to 12% lower than the splitting tensile strength (Neville, 1996).

The static elastic modulus of Mix 111 was 13.8 ± 0.9 GPa. This compares with 14 to 42 GPa for normal weight concrete and 7 to 28 GPa for cement paste (Mindness and Young, 1981). The static Poisson's ratio was determined to be 0.21 ± 0.2. The value for concrete is typically in the range of 0.15 to 0.22 (Neville, 1996).

4.8 Ultrasonic Pulse Velocity

As shown in Figure 7, the P-wave velocity of Mix 111 grout decreases with decreasing moisture content. The initial velocity of 4.14 ± 0.09 km/s in the saturated condition falls within the range of 3.5 to 4.2 km/s for saturated mortar (Neville, 1996). The P-wave velocities in different rocks ranges from 1.4 to 6.5 km/s depending on type (Roberts, 1977). The acoustic impedance of Mix 111 also depends on moisture content and was measured to be $8.84 \times 10^6 \pm 3.2 \times 10^5$ kg/m^{2}s after wet curing for 28 days.

4.9 Thermal Resistance

The thermal resistance tests conducted at the University of Alabama showed that the experimental resistance was lower than the calculated. The grout mix with higher superplasticizer dosage had lower resistance in the cooling mode and higher resistance in the heating mode than the other mix. Thermal resistance did not appear to be greatly affected by contraction of the U-loop at low temperatures during the heating mode tests.

The tests did not account for contact resistance between grout and surrounding ground. This would be a useful extension of the thermal resistance studies. Also, the rig could be used to determine the effect of repeated operating cycles on grout performance.

5.0 FIELD TRIALS

5.1 Oklahoma State University

The first field trial was conducted at Oklahoma State University (OSU) in Stillwater in August. The depth of the groundwater table at this site is approximately 20 ft. Two 260 ft deep boreholes were drilled by Geo Energy Drilling. The first of these was 5 in. diameter and the second was 3⅝ in. diameter. A 0.75 in. diameter U-loop was used. A 1 in. diameter tremie tube was taped to the U-loop and a steel weight bar was attached to the end of the loop. The end of the tremie tube was taped and a small hole was cut in the side of the tube. Thermistors were attached to spacers on the U-loop to measure temperature at the grout/borehole wall interface at various depths. Figure 9 shows the thermistors. The spacers were designed to fold and keep the U-loop centralized within the borehole. Figure 10 depicts the loop and tremie tube being inserted into the borehole.

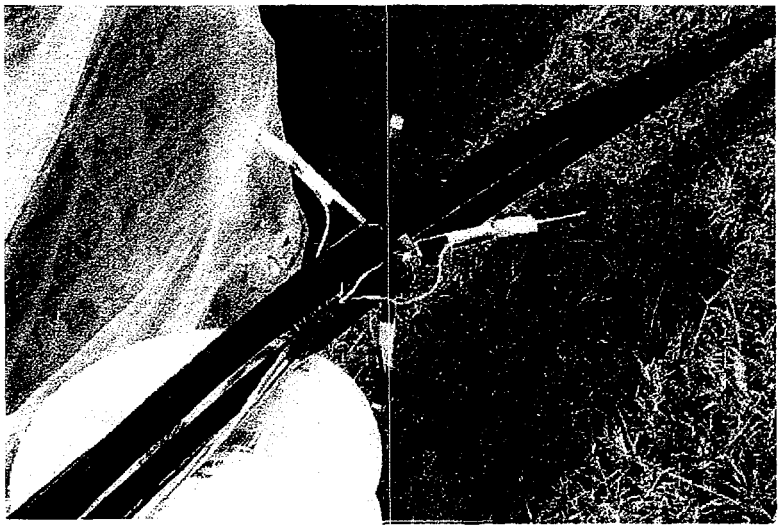

Figure 9. Thermistors attached to U-loop.

The grout was mixed in a 34 gallon capacity ChemGrout paddle mixer. This is the same type of mixer used in preliminary tests at Brookhaven. The OSU mixer had a Moyno pump where as the BNL rig uses a piston pump. For cement-sand grouts a ram or piston pump is preferable since wear on a Moyno pump may be excessive. A batch of grout consisting of one bag of cement to two bags of sand was mixed. The amount of water added was 6.19 gallons giving a water/cement ratio was 0.55. The superplasticizer dosage was 639 ml/batch. The mix proportions correspond to those in Table 5 except that the bentonite was omitted. This grout formulation had been mixed several times

in the paddle mixer at Brookhaven before the field trial. The batch volume was approximately 19 gallons.

Figure 10. U-loop and tremie tube being inserted into borehole at OSU.

The grout mixed at OSU appeared very fluid and the first batch was successfully pumped. The tremie tube was gradually withdrawn as grout was pumped. The specific gravity of a sample was measured and found to meet the specification of 2.18. However, it was observed that while the grout was immobile in the hopper sand had a tendency to settle out and cake at the bottom. The second batch of grout was mixed and the pump was re-started after an interruption of a few minutes. During this interval the tremie tube apparently plugged and the grout could not be pumped through the tube although it could be pumped directly out of the hopper. Again, excessive segregation of sand appeared to be occurring. This problem had not been encountered previously at Brookhaven and it is not clear why it occurred with an identical mixer and mix proportions. The segregation of sand resulted in a non-uniform, unstable grout. Where the solids had settled and caked the material was hard and dense. This gave the false appearance that the grout may have set. However, the set time of the grout is several hours even at high temperatures and this was not a plausible explanation.

OSU later constructed an arrangement whereby the grout could be continuously mixed and pumped so that there were no interruptions to the pumping. The two boreholes were then successfully backfilled.

Several important lessons were learnt from the OSU field trial. The first of these is the importance of a relatively stable grout, i.e., one that does not excessively bleed or segregate. While the mix proportions appeared suitable in the preliminary tests at Brookhaven it was clear the same grout at OSU exhibited different characteristics. Use of an additive such as bentonite, alteration of the mix proportions or use of high shear mixer can remedy this problem. Further tests on mixes containing bentonite were conducted at Brookhaven prior to the field trials at Sandia. This is discussed below.

The second important point is the need to keep the grouting operation as continuous as possible. Grout plants used in geotechnical and other applications that employ cement-sand grouts typically consist of one mixer tank and one agitator tank. After the grout is mixed (in either a high or low shear mixer) it is transferred to the agitator tank where it is continuously stirred. This prevents or minimizes any segregation of solids. The grout is pumped from the agitator tank while the next batch is mixed. In this way pumping is not interrupted while waiting for the next batch of grout and the risk of plugging lines is reduced. These types of plants are commercially available and recommended for future use of cementitious grouts in GHP applications. This would also speed the grouting process. It is also important that a large capacity mixer be used to minimize the number of batches that have to be mixed.

The thermal performance of the cement-sand grouts and the staff at OSU is monitoring conventional bentonite grouts at the same site. The results will be reported later when they are completed.

5.2 Sandia National Laboratories

Sandia purchased a ChemGrout CG 555 45 gallon paddle mixer for the field trials in Albuquerque. The mixer was equipped with a 30 gallon holding hopper and a piston pump. In preparation for the field trials Mix 111 was re-formulated to include bentonite. Tests were performed at Brookhaven to confirm that the grout was pumpable. Figure 11 shows the grout being pumped through a tremie tube to fill 20 ft long, 4 in. diameter PVC tubes each containing a single 1 in. U-loop.

The site at Sandia is arid with the groundwater table at a depth of approximately 480 ft. A total of five boreholes 250 ft deep and 4 in. diameter were drilled by Geo Energy Drilling. The boreholes were approximately 35 ft apart. A 1 in. diameter U-loop was used in each of the boreholes. No special efforts were made to centralize the U-loop. Hence, some wandering throughout the length of the borehole can be expected. The tremie tube used was 1.25 in. diameter and the end of the tube was kept open. A small hole was also cut in the side of the tube. Two boreholes were completed with cement-sand grout, one with Benseal bentonite grout and the other two were used

by Baroid to test one of their grouts. The first borehole backfilled with Mix 111 used Type I cement and the second borehole used the same grout with Type V (sulfate resistant) cement. Type V cement has a lower exotherm than Type I and the purpose of its use was to determine whether there was any benefit.

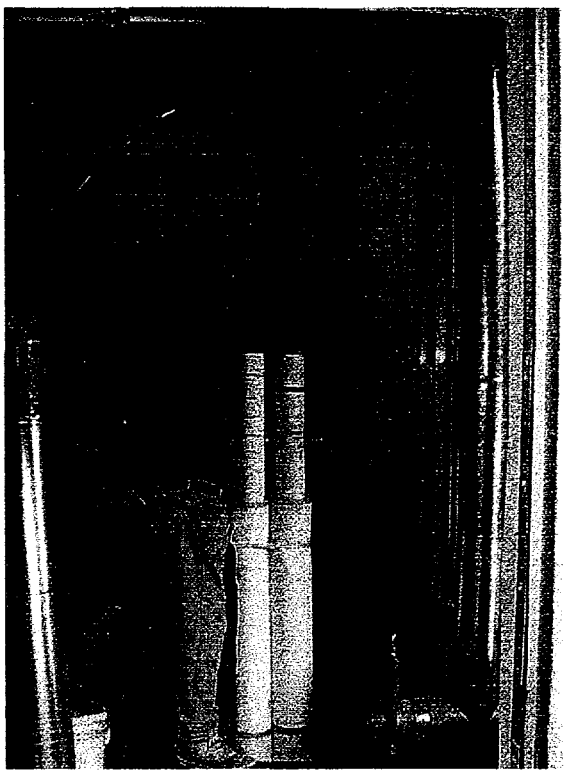

Figure 11. Pumping grout into 20 ft tubes containing U-loop at Brookhaven.

The larger grout mixer allowed preparation of a larger batch of grout than was possible at OSU. Each batch of grout consisting of two bags of cement to four bags of sand was mixed. The amount of water added was 12.4 gallons giving a water/cement ratio was 0.55. Bentonite was added at a rate of 936 g/batch. The initial superplasticizer dosage was 1200 ml/batch. This was later increased to 1400 ml/batch to improve pumpability. The batch volume was approximately 38 gallons and this filled the mixer tank.

Prior to mixing the grout approximately 13 gallons of water was pumped through the tremie tube to lubricate the lines and remove any mud or material that might be blocking the outlets. The addition of extra water to the borehole may change the final composition of the grout in the bottom of the hole. However, it was felt that ensuring that the tremie tube was unblocked before pumping the grout was necessary.

The required amount of water for each batch was measured out into 5 gallon buckets. A total necessary for four batches was measured and set up close to the grout mixer. Bentonite (Aqua Gel, Baroid) was added to the water and mixed using a Jiffy mixer attachment on a drill. Once the bentonite was well distributed the required volume of superplasticizer was added. Premixing the bentonite and superplasticizer reduced the amount of time for which the grout mixer was needed. The premixed water, bentonite and superplasticizer were then added to the mixer tank. The cement was mixed for several minutes to ensure it was well dispersed and free from any lumps. Sand was then added and mixed for several minutes until the grout was visibly uniform. The specific gravity of the grout was measured to check that it was within limits. The grout was then gradually added to the hopper and pumping commenced. The tremie tube was slowly withdrawn as the grout was pumped. Occasionally the grout in the hopper was agitated using the Jiffy mixer to keep it relatively mobile. Unlike the grout mixed at OSU, the grout at Sandia did not tend to segregate and this is attributed to the use of bentonite.

As soon as the mixer tank was emptied the next batch of grout was mixed and the process repeated. There was usually a few minutes interruption in pumping while the subsequent grout batches were prepared. However, no problems were encountered when re-starting the pump and backfilling easily proceeded. Four batches were used to fill each borehole. There was little difference in the pumpability of the grouts prepared from Types I and V cement. The grout height in the first borehole decreased about 6 ft one hour after filling and was later topped up. The second borehole also saw a decrease in grout height and this may have been due to loss of grout to the surrounding formation. A gravel layer was encountered at a depth of approximately 40 ft while drilling and this may have acted as a loss zone.

Benseal (Baroid) bentonite grout was used to complete one of the boreholes and form a baseline comparison for the cement-sand grouts. For each batch of grout 30 gallons of water was added to the mixer and a small cup of New-Drill polymer added to retard gelling. A 50 lb. bag of Benseal was then mixed in and the grout was pumped through the tremie tube. Four batches were used to fill the borehole.

Figures 12 to 15 show the various stages of drilling, loop installation and grouting process.

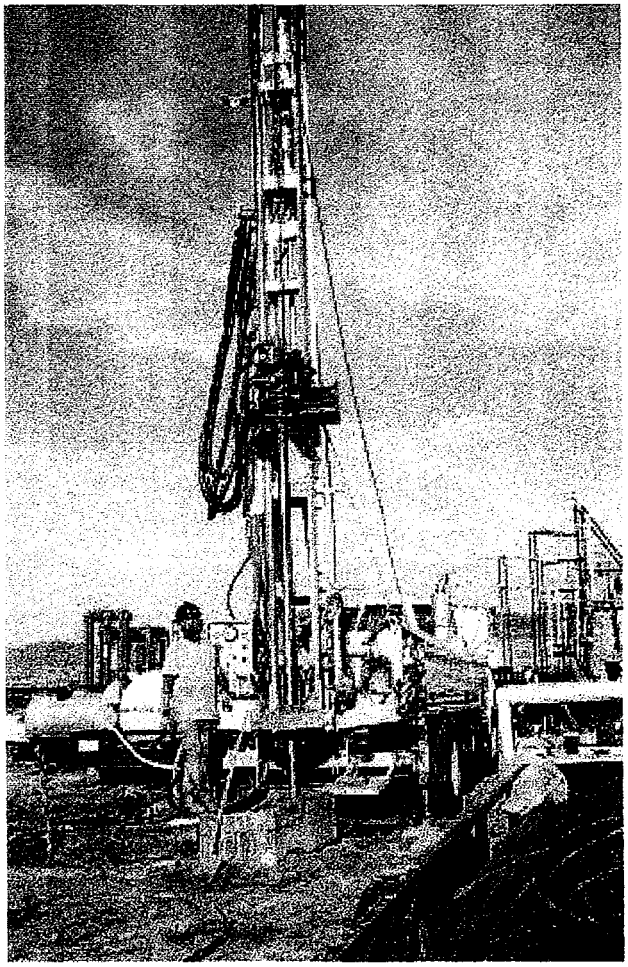

Figure 12. Drill rig used at Sandia field trial.

Figure 13. Installing loop at Sandia.

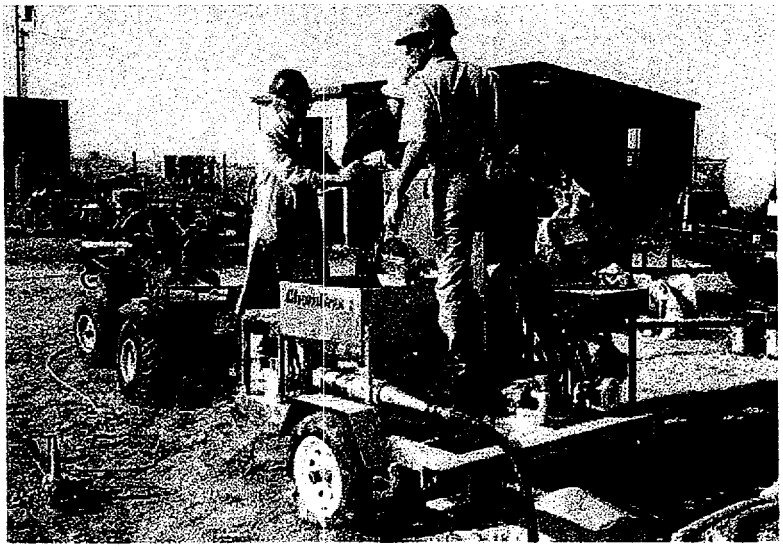

Figure 14. Mixing grout at Sandia.

Figure 15. Mixing grout at Sandia. Photo shows grout being transferred from mixing tank to holding hopper.

The problems of plugging the tremie tube that were encountered at the field trial at OSU were overcome at Sandia and the latter trial was very successful. The major differences were: (1) addition of a small quantity of bentonite to the grout; (2) occasionally agitating the grout in the hopper; (3) mixing the grout in a larger batch; (4) use of a piston pump; (5) use of a 1.25 in. diameter tremie tube and (6) flushing the tremie tube with water prior to pumping grout.

It is still recommended that a grout plant with separate mixer and agitator tanks be used to prevent interruption in pumping. Use of a high shear colloidal mixer may obviate the necessity for using bentonite in the grout and may also permit reduction of w/c and superplasticizer dosage. Furthermore, repeated lifting of the 100 lb. bags of sand and 94 lb. bags of cement is very energy intensive, particularly in hot weather. Mixing would be easier and quicker if the dry ingredients were preblended and packaged in 50 lb. bags. The superplasticizer is available in powdered form so it could be preblended also. Preblending and packaging the dry ingredients is expected to increase the cost of the grout significantly. Therefore, the convenience and reliability of using the grout in prepackaged form introduces additional cost.

6.0 FEASIBILITY OF NON-DESTRUCTIVE TESTING

Non-destructive tests offer the potential to verify bonding integrity and quality of grouting in-situ. Since GHPs operate primarily by conduction, their performance depends highly on the thermal conductivity of the backfill material. Furthermore, preliminary evaluations suggest that ensuring good thermal contact at all interfaces: (a) between the U-tube and backfill material and (b) between the backfill and the soil is also of primary significance for the successful operation of GHPs. Such considerations are important to facilitate the heat transfer process. During the cooling mode of operation heat is transferred to the surrounding formation. This process can cause moisture to migrate in the vicinity of the ground heat exchanger thus altering the soil conductivity. Similarly, it has been recognized that wet/dry cycling of the soil around the heat exchanger may result in formation of gaps that in turn influence the heat transfer process. Current in-situ heat transfer tests cannot distinguish between changes in grout or soil conductivity and the formation of gaps due to dimensional changes that introduce contact resistance into the system. If an appropriate test could be developed to monitor changes in dimensions and bond integrity this would enable better comparison of in-situ performance of different grouting materials. Furthermore, in-situ tests to assure that the borehole is completely grouted would be very valuable both from heat transfer and environmental standpoints.

As discussed previously, interface conditions have recently been looked upon from a different frame of reference: environmental considerations. Among others, Minnesota and New Jersey state environmental authorities have been concerned with potential gaps that might be responsible to facilitate communication between aquifers encountered along the depth of the vertical ground heat exchangers. They postulate that such gaps could lead to environmental risks e.g., contaminated surface or ground waters might migrate to the aquifer. Similarly, another issue of concern is cross contamination among aquifers that might be facilitated by the vertical boreholes of the ground heat exchangers. It is reasonable to expect that the presence of gaps will change the hydraulic conductivity (permeability) thus increasing the seepage along the depth in the vicinity of the vertical heat exchanger. The results obtained for grout/pipe specimens confirm that interfacial conditions do impact the system permeability. However, without necessary in-situ testing on actual grouted boreholes and/or seepage analysis, it is difficult to judge the significance of postulating such scenarios. Some experimental and numerical results exist (Edil et al., 1992) for the sealing of water wells. They can provide a general guidance on the relevant issues. However, one should recognize that fundamental differences exist between the respective configurations. Therefore, it is recommended that similar studies be performed to investigate the sealing characteristics of the GHPs.

In addition to concerns that may arise from the operational loading and other external conditions, construction of the ground heat exchangers may result in imperfections that can have adverse effects on their functionality. Because the ground heat exchangers are underground structures it is generally difficult to verify the in-situ condition in terms of geometry or material properties. We are especially uncertain about the status of the bonding between the various

components. Verification of the bonding between the various components of the heat exchanger borehole is very important since it is directly related to the heat transfer process. Furthermore, model development for the heat conduction in the system is based on perfect thermal contact between the components (see e.g., Gu and O' Neal, 1998). It has been recognized that even for the perfect bonding condition, it is very difficult to obtain an exact solution for the transient thermal response problem. BNL is currently working on modeling imperfect bonding by assuming the presence of gaps along the pertinent interfaces. The latter work is based on finite element modeling of the heat transfer problem related to the ground heat exchanger. This is discussed further in Section 7.0. It is expected that the heat transfer between the heat exchanger and soil can be reduced significantly lower due to debonding both in terms of distribution as well as magnitudes.

The above are different aspects describing the general need to develop validational tools for verifying the in-situ condition of the ground heat exchangers of GHPs. The consensus within the geothermal pump industry is that the development of such techniques will be very useful in addressing issues related to the reliability, the long term performance as well as the design and construction of GHPs. In response to this need, BNL has begun a study to investigate the feasibility of employing non-destructive methods to verify in-situ conditions along the vertical ground heat exchangers of GHPs. This effort is combined with systematic engineering evaluations of relevant field conditions. Such evaluations will be used to support testing setup, procedures and, in particular, for the interpretation of field results.

6.1 Backfill Requirements

The primary function of the backfill in geothermal heat pumps is to facilitate the heat transfer process between the heat exchanger and the surrounding formation. The creation of various gaps at the interface due to either the operation of the heat exchanger, backfill shrinkage, thermal contraction of HDPE U-tube, or external conditions leads to an appreciable reduction of the overall conductivity of the system. Heat rejection by the heat exchanger could produce moisture migration into the soil. Similarly, the soil in the vicinity of the heat exchanger can become dry due to heat absorption. Sharp variations of the soil moisture content and subsequent shrinkage may result in loss of bonding and consequently reduce the effectiveness of the geothermal heat pump. Therefore, by requiring favorable heat transfer in the system, one needs to address the issue of the thermal conductivity of the backfill material itself as well as the issue of backfill bonding. Accordingly, we can state that the important aspects of the backfill are:

1. The backfill must have favorable thermal conductivity.
2. The backfill must be coupled to the U-tube.
3. The backfill must be coupled to the formation.

Backfill bonding is a very important aspect of the functionality of the ground heat exchangers. Ideally, the backfill material must:

1. have competent density as per design requirements, and
2. fully surround the pipe

These requirements are illustrated in Fig. 16(a). However, in-situ conditions can be significantly different. Examples of undesirable in-situ conditions are schematically shown in Fig. 16(b). Four possible material cases are presented:

1. competent density backfill, i.e., uniform, bonded grout,
2. mixed density (inhomogeneous) backfill reflecting unintended variations of backfill generated by inadequate mixing or placement problems,
3. air gaps, and
4. fluid-filled gaps.

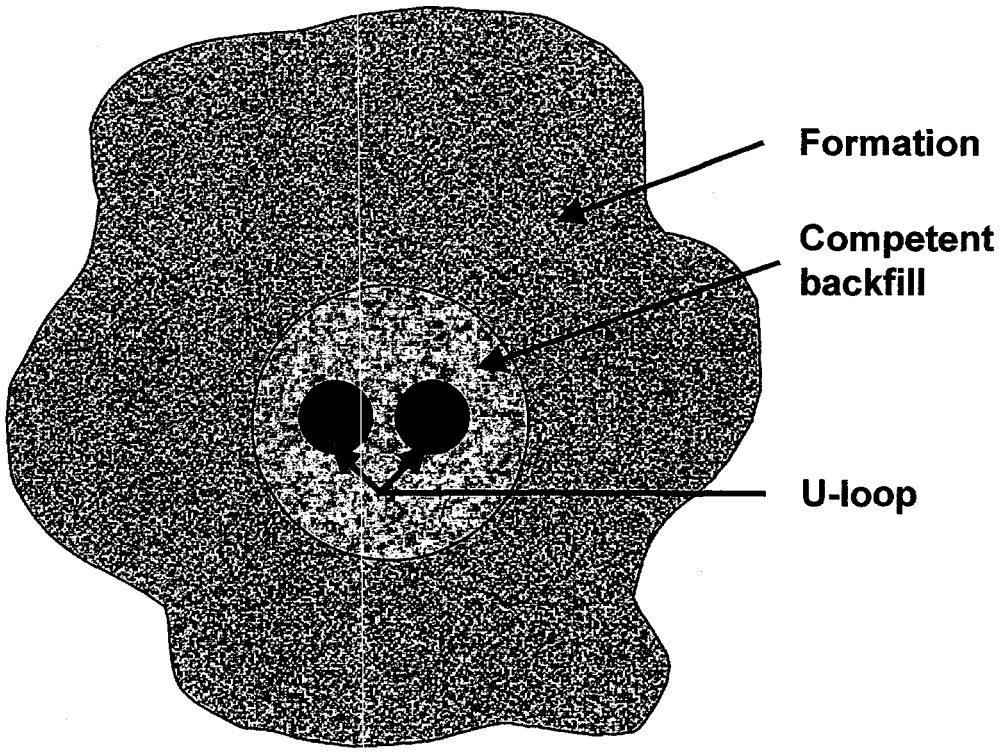

Figure 16a. Section of Ground Heat Exchanger Showing Acceptable Condition.

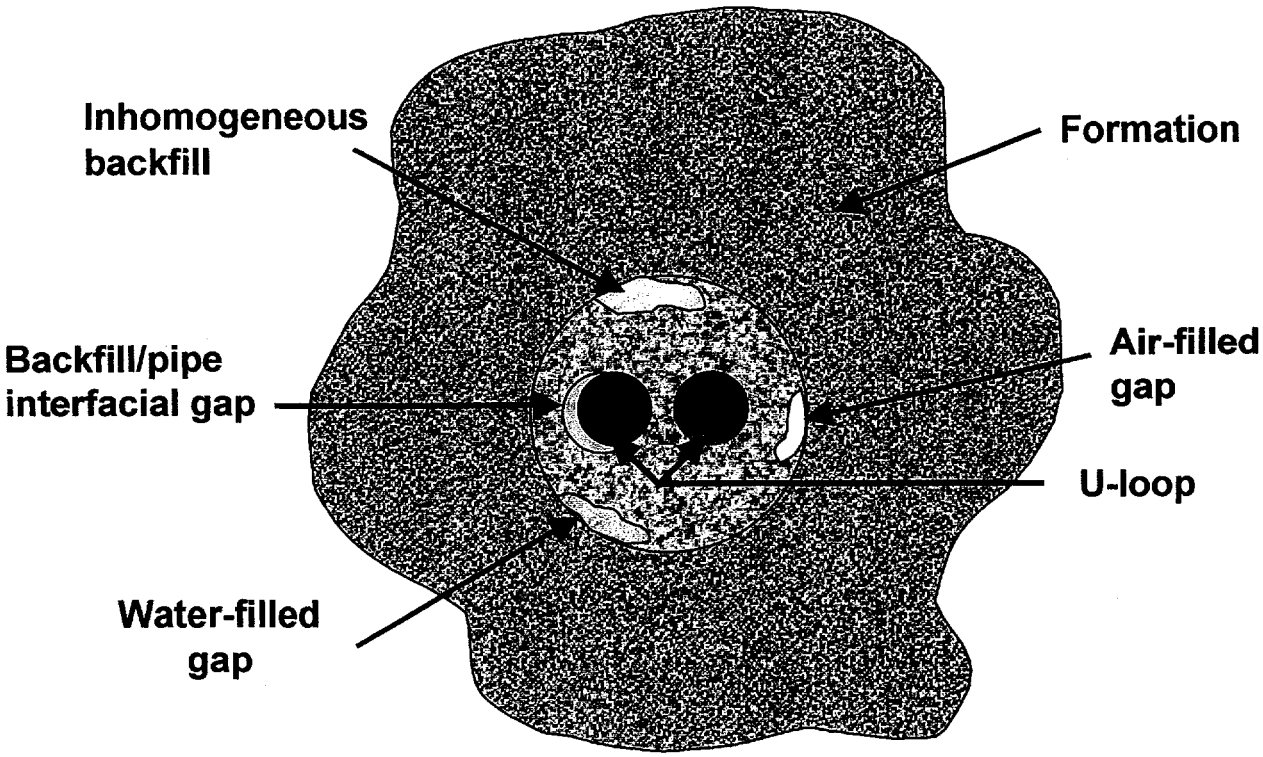

Figure 16b. Section of Ground Heat Exchanger Showing Undesirable Conditions.

The above discussion demonstrates that thermal conductivity is not the only determining factor for the reliability of GHPs. Additionally, it must be demonstrated that backfill-bonding requirements are met. This means that continuity between backfill and pipes as well as between backfill and formation must be ensured.

So far, it has been argued that backfill bonding is important with regard to heat transfer. There are, however, other equally important factors to impose such requirements. Specifically, as mentioned above, local environmental regulators (i.e., state authorities) have been concerned with the possibility of vertical leakage in the ground heat exchanger borehole. Lack of backfill bonding can result in the formation of gaps or channels that can be responsible for the creation of potential paths for leakage of contaminants. It is postulated that vertical leakage can cause contamination of fresh water aquifers or cross contamination between aquifers. Such concerns have generated considerable delays that have made a negative impact in the geothermal heat pump industry. In several instances, construction of geothermal units has been stopped until such issues are resolved. This obviously has an adverse effect on the growth of geothermal heat pump technology. Similar concerns have been posed by the US Environmental Protection Agency (EPA) with respect to the integrity of a variety of wells used by the petroleum industry. Furthermore, similar concerns have been expressed for the case of industrial waste injection wells.

Injection wells in oil fields are required by the EPA to demonstrate adequate cement bond involving the casing as well as the formation. For this purpose, a variety of cement bond evaluation logging tools are currently available that are based on sonic and ultrasonic measurement techniques (see e.g., Jutten et al., 1993, Albert et al., 1988). A section of an oil well is shown in Fig. 17. In view of this configuration, the cement has two key roles:

1. provide support for the casing
2. provide complete isolation of the borehole annulus

Some argue that supporting the casing it is not as critical as its function to minimize leakage. In order, however, to provide these functions, the cement must satisfy the following requirements:

1. must be acoustically coupled to the casing
2. must be acoustically coupled to the formation
3. must be fully occupy the annulus between the casing and the formation

The first two of these requirements enforce continuity at the cement/pipe and cement/formation interfaces. Microannuli filled with gas or fluids should not be present. A microannulus is a small gap between the casing and the cement. They usually occur when the pressure inside the pipe is released after cement setting. Temperature and pressure changes are believed among the reasons causing such microannuli.

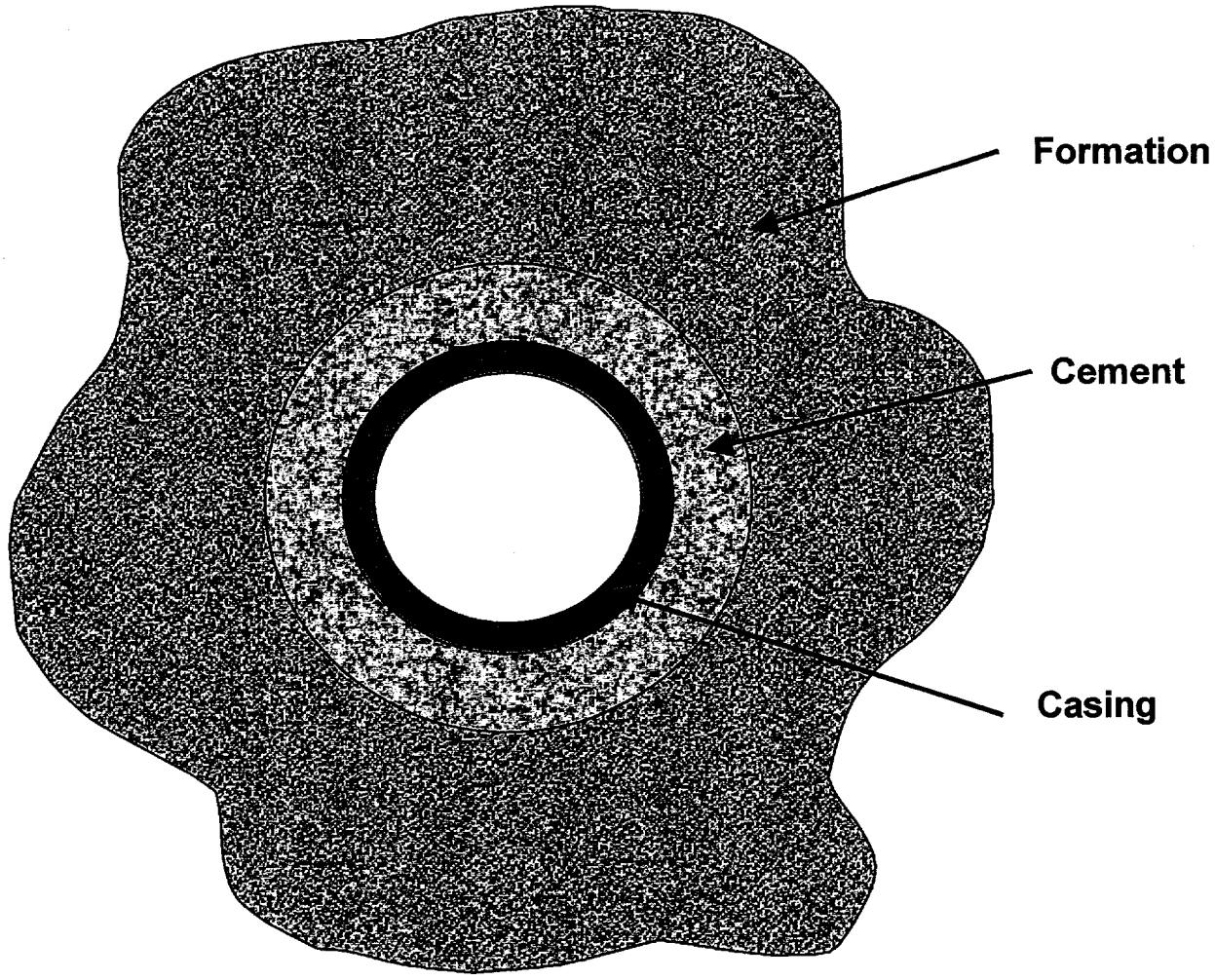

Figure 17. Section of Cased Well.

By comparison, one can identify similarities between requirements for the geothermal heat exchangers and oil wells. It is clear that bonding is a key factor in both cases. For the former case such bonding is required:

1. to facilitate heat transfer
2. to prevent vertical leakage;

Whereas in the latter case the requirements are:

1. to provide structural support
2. to prevent leakage

It is reasonable, therefore, to look into the various bonding and material quality verification methodologies and field measurements which for about forty years have been employed by the petroleum industry. Some of them have a good potential to be applied for the verification of ground heat exchangers of GHPs. In addition, other methods of non-destructive testing (NDT) used in geotechnical application and soil-structure interaction verification will be considered for the same purpose. Field verification is a significant aspect of the geothermal pump industry's efforts to address regulatory issues. Therefore, it is expected to support the process of promoting the application of the geothermal heat pump technology to residential and commercial buildings.

6.2 Acoustic Techniques

A widely used approach to obtain material information in different wells is through acoustic or sonic logs. The general principle involves the generation of sound waves using a magnetostrictive or a piezoelectric transducer and consequently the measurement of the response by one or more receivers. The response contains information about the material properties such as the porosity of the medium. The transducers typically produce waveforms with average frequency in different ranges depending on the particular nature of the technique (low frequency is typically in the neighborhood of 20-40 kHz while high frequency is usually at about 500 kHz). Their duration is short but they are repeated ten to sixty times per second.

A typical source signal is shown in Fig. 18(a). It is important that the well is filled with water or mud so that the transmitter becomes coupled with the borehole wall. Most sonic probes have one or more receivers that are selectively spaced at certain intervals apart. This allows for a better recording of the response signals. Also, some probes are equipped with two transmitters. This depends on the particular design of the sonic probe. A typical configuration has one transmitter coupled with two receivers. Such system is schematically displayed in Fig. 18(b) together with some notation relevant to the definition of transit-times.

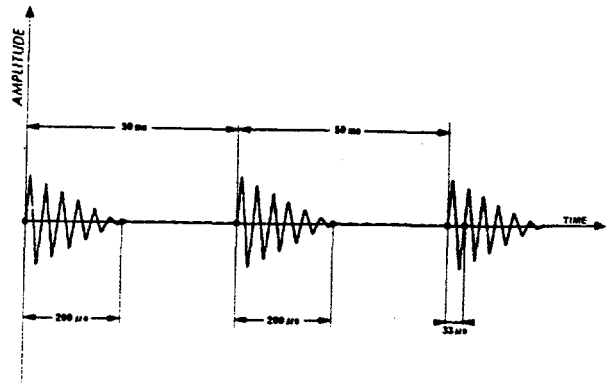

(a)

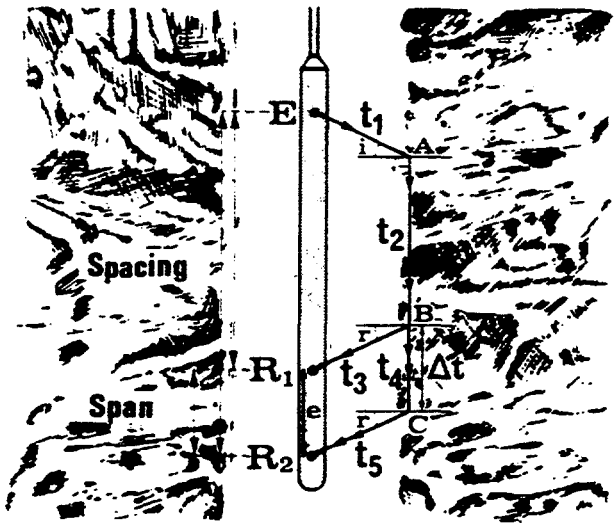

(b)

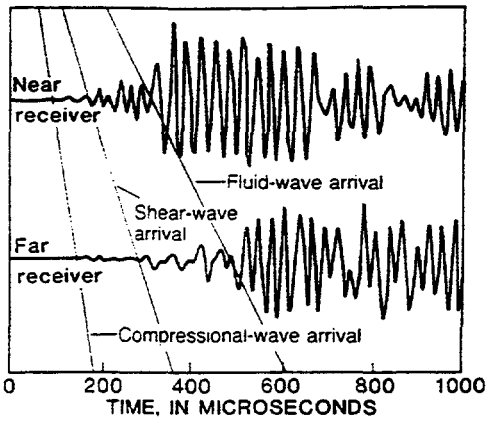

(c)

Figure 18. Acoustic Methods: (a) Source Signal, (b) Source-Receiver Arrangement, and (c) Waveform Arrivals (after Serra, 1984).

In Fig. 18(b), a spherical wave is generated at the source (point E). After its initial propagation through the water or mud, the wavefront strikes the surface of the borehole. This incidence produces reflected as well as refracted waves. Their nature depends on many factors, primarily, the angle of incidence and the acoustic properties of the formation. The propagation from the transmitter through the water or mud involves P-waves since the latter media do not propagate S-waves. Thus, the incident wave is a P-wave which produces reflected and refracted P- and S-waves depending on the angle of incidence. Using simple theory from the incidence of body waves at the surface of a halfspace, then when the incidence angle is less than the critical, the incident P wave produces a refracted P-wave and reflected P- and S-waves, respectively. A general description of the wave propagation pattern in a well with a one foot diameter is shown in Fig. 19. The well is drilled in a very stiff formation (wavespeed of compressional waves equal to 20,000 fps while the corresponding wavespeed in the mud is 5000 fps).

When the angle of incidence of the P-wave is larger than the critical, then all that is generated is a reflected P-wave. The response at critical angles consists of propagation along the borehole wall thus producing secondary sources. Refracted waves propagate from the source through the fluid or mud and are refracted at the borehole wall, travel through the formation and then refracted again through the fluid and consequently recorded at the receivers. There is another type of wave generated in the borehole, namely, guided waves. The latter propagate in the borehole fluid or at the interface between the borehole wall and the fluid. Ultimately, waves generated by the transducer reach the two receivers R1 and R2, respectively. The time that elapses between the response signals to arrival at these two receivers is recorded to produce transit-time logs. It can be shown that the transit time is equal to the distance of the two receivers divided by the wavespeed in the formation. Thus, the difference in time of arrival at the two receivers is converted to transit time and appropriately recorded. The transit time for the arrival of the P-waves is easily identified because P-waves travel faster than S-waves (they arrive first at the receiver and they can be clearly distinguished from background noise). S-wave arrivals are separated from those of P-waves. They are followed by the fluid-wave arrivals. Waveforms from compressional, shear and fluid wave arrivals at a two receiver system are shown in Fig. 18c.

Sonic tools usually record these waveforms in their entirety, not only their respective arrival times. They are recorded digitally, and time history representations can be obtained through an oscilloscope. This allows for a better interpretation of the sonic logs. Specifically, digitized records of the respective waveforms can be used in a variety of analyses. For example, digital records can be corrected due to recording errors or other discrepancies. Additionally, having digitized records of the acoustic measurements one can construct the respective frequency and amplitude plots required to give a more complete characterization of the borehole response. Amplitudes as well as wave attenuation are very important quantities for the characterization of the formation.

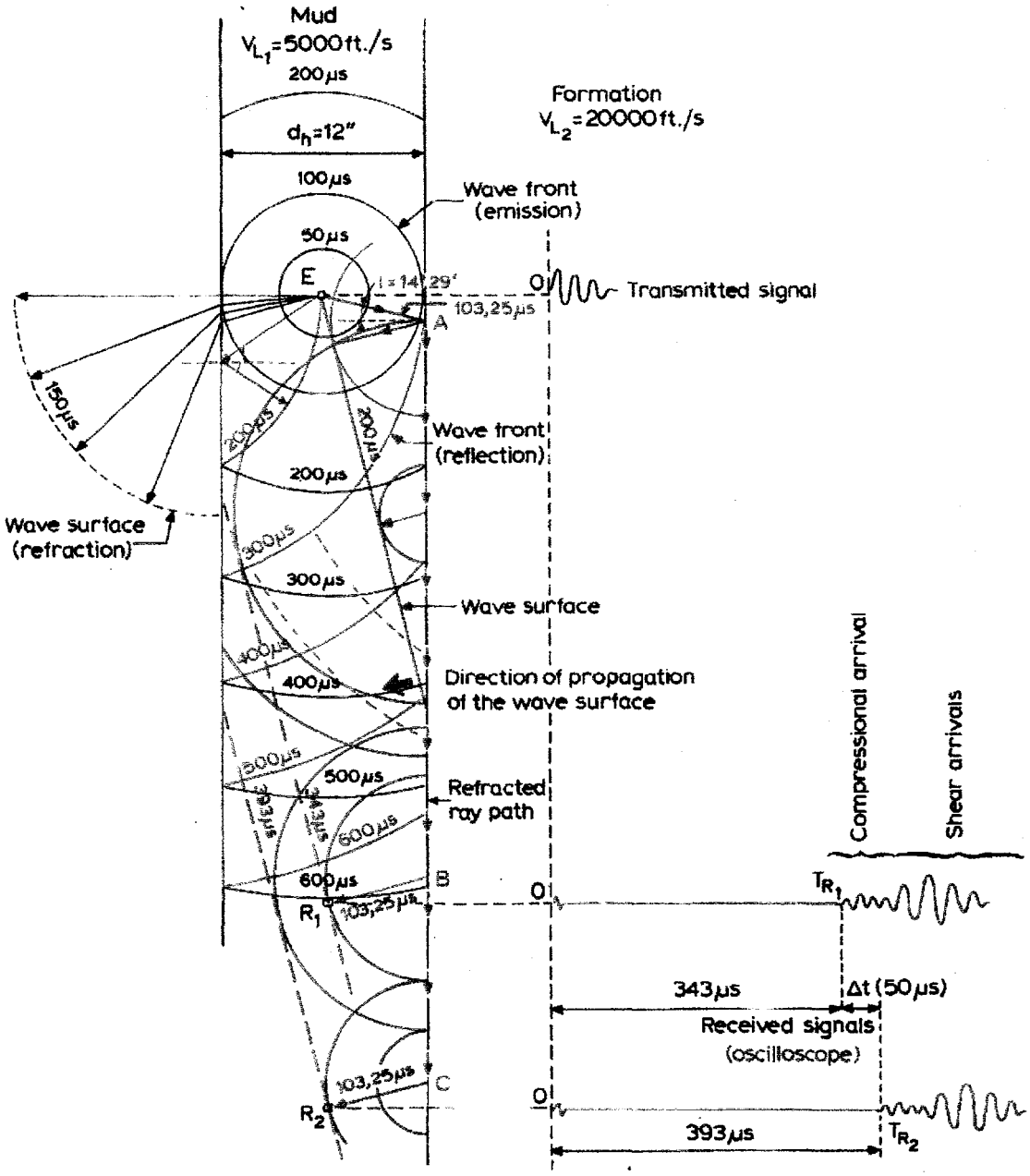

Figure 19. Propagation Patterns in a Well (after Serra, 1984)

Some of the known factors that are responsible for errors in acoustic measurements are geometric in nature. It was discussed above that sonic logs are obtained on the basis of principles of wave propagation. If the assumptions underlain these principle are not met, then errors occur. One of the problems arises when the surface of the borehole wall is not smooth e.g., when caves exist. Another common source of error is generated when the axis of the sonic tool does not coincide with the axis of the borehole. In order to minimize the effects from such error sources, tools containing additional transducers and recorders are employed. In the latter case, transit times are determined as averages.

As indicated above, the wavespeeds recorded by acoustic methods are affected by several factors. Primarily they depend on the geometry and the material properties of the borehole wall. Porosity and fluid content are significant factors. In general, the higher the porosity the lower the wavespeeds recorded by acoustic techniques. Temperature and pressure affect the state of the pore fluid and consequently the wavespeeds of propagation. Another important factor is the continuity or potential anisotropy of the material. Treating the material surrounding the borehole as a continuous medium may not be applicable if the formation is cracked. In the latter case, certain wavelengths cannot be transmitted through the formation. The presence of microfissures in the formation has been though to be the reason that in certain media wavespeeds recorded by acoustic logs did not match those obtained from seismic surveys.

At sites where water tables are of interest, acoustic methods were very effective in detecting water table depth. Other commonly used logs such as neutron, gamma-gamma and resistivity were not as direct. Most recent analysis of propagation of acoustic waves in a borehole, the material is treated as a two-phase medium. The propagation in the matrix material becomes coupled with that in the pore fluid. This is done on the basis of Biot's theory (Biot, 1956). The coupling is due to the dilatation. Such coupling takes into account the compressibility of the pore fluid. In addition, attenuation due to losses in the matrix material as well as due to the flow of the pore fluid can be incorporated. A two-phase approach can be used to explain some of the differences between dynamic responses in dry and saturated formations (Philippacopoulos, 1997, 1998).

6.2.1 Cement Bond Logging

Among the most known applications of acoustic techniques in the field of cement evaluation is the Cement Bond Logging (CBL). Over the last 30 years, it has been used throughout the world with various degrees of success. Several improvements have been made to facilitate its use in the field. A typical CBL is carried out using a sonic tool that emits a 20 kHz P-wave that, after propagating in the mud or fluid, is incident upon the casing. The transmitter and the receiver are typically omnidirectional, a feature that represents one of the drawbacks of the method. In response to the CBL acoustic signal, the casing vibrates in a plate-type mode. For wavelengths comparable to the thickness of the steel, the propagation speed approaches the compressional wavespeed in the casing material. When the bonding between the casing and the cement is good, then, by traveling parallel to the borehole axis, the response is attenuated due to shear coupling between the steel and

the cement. When fluid is located outside the casing, then this attenuation is small. Therefore, the response amplitudes at the receiver depend on the presence of cement around the casing. This becomes the basis of the method. In general, high amplitudes imply low attenuation which in turn signifies poor bonding. Low amplitudes imply high attenuation and consequently good cement bonding. Obviously, these are general guidelines. Interpretation of the particular amplitudes of the wave arrivals is a complicated matter due to many factors that are influencing input-output relationships of this configuration.

Theoretically, the compressional waves generated by the transducer are propagated through the mud, casing, cement sheath and formation. Sequential reflection and refraction produces a variety of body and interface waves. Backward propagation through these media produces a set of waves that ultimately arrive at the receivers. The recorded responses contain information about the properties of all components involved, as well as information pertaining to the interface conditions between them, namely acoustic coupling. Of particular interest are the observed attenuation, the frequency content and the arrival times at the receivers. Breaking down the total response to specific components is a subject of interpretation. A set of generic receiver waveforms (total signal obtained at the receiver) is presented below. They reflect bounding type situations with respect to interface conditions and are of significant importance in the interpretation of field measurements.

One of the bounding cases is associated with complete absence of cement from the composite borehole. Accordingly, the pipe is free to vibrate within the borehole (free casing). Because of zero coupling with the formation, the receiver waveform is essentially the casing response. This is schematically shown in Fig. 20(a). Another bounding case corresponds to a complete acoustic coupling between all of the system components. The cement is considered to fill completely the annulus between the casing and the formation, (considered uncontaminated and without any voids). The acoustic coupling of the cement with both the casing as well as the formation is perfect. In such an ideal case, the response waveform at the receiver is expected to be dominated by the response of the formation. This is schematically shown in Fig. 20(b). Since the system is now acoustically stiffer than that of the previous case, we see a shift to higher frequencies.

As indicated, the above two cases i.e., free-casing and full-coupling essentially represent bounding cases. In the former case the annular space is considered uncemented whereas in the latter case it is completely filled with competent cement material. Some intermediate cases are illustrated in Figs. 20(c) and (d). In Fig. 20(c), there is no bond between the cement and the formation while the cement to pipe interface is considered as fully acoustically coupled. Because of the latter coupling, the pipe is stiffened by the cement and therefore the free casing frequency cannot be detected at the receiver. On the other hand, due to the acoustic isolation of the combined pipe-cement system with the formation, the formation frequencies are not presented in the total response waveform recorded at the receiver.

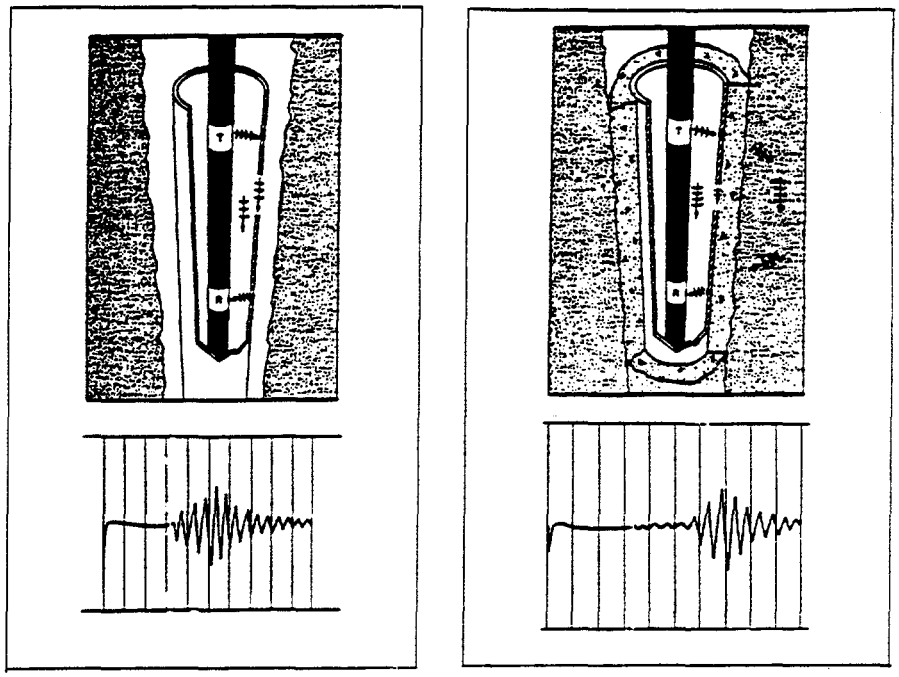

(a) (b)

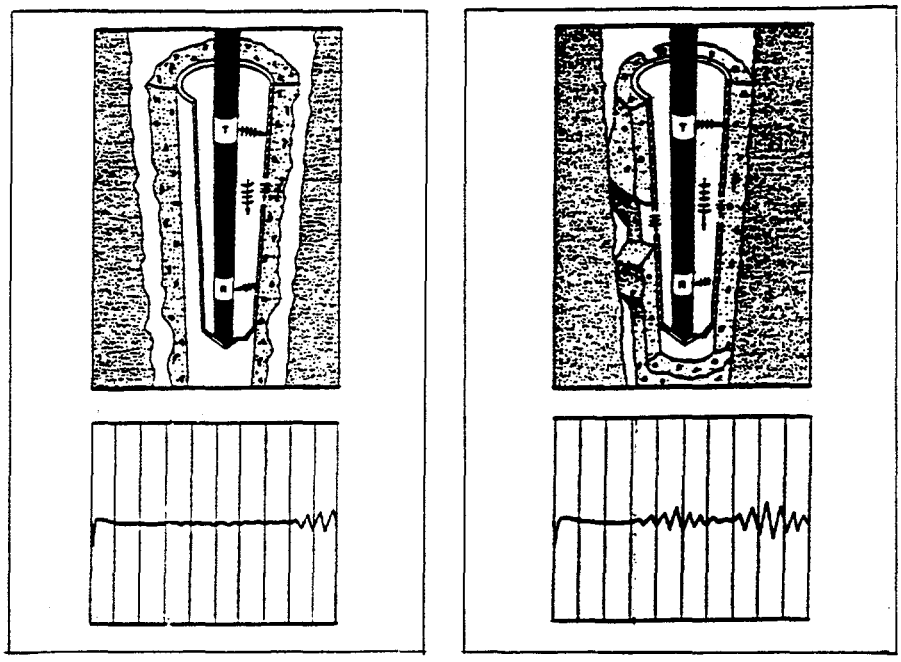

(c) (d)

Figure 20. CBL Receiver Signals (after Goodwin and Carpenter, 1991).

Finally, Fig. 20(d) displays a case characterized by the presence of channels between the cement and the formation. In addition, microannuli exist between the cement and the casing. When loss of contact exists between the casing and the cement, then the casing can vibrate locally and therefore the casing frequency will be present at the total response signal. Conversely, when good contact exists between the cement and the formation, then the formation signal will be predominant. On the basis of the preceding analysis, the case of a microannulus can be distinguished from that of channeled cement whereby the channel is in contact with the casing. All that is required is to pressurize the casing. If after doing so, the casing signal still appears in the response waveform, the likelihood of presence of a channel in contact with the casing is very high (the deformation due to the pressure should be able to close the gap due to the microannulus thus eliminating the casing frequency from the response signal).

The above are generic combinations of interface conditions between the two key interfaces of the pipe-cement-formation system. Field conditions are more complex in the sense that the spatial variability of interface conditions can be completely random. By that it is meant, both circumferential variations as well as variations along the depth (i.e., along the axis of the borehole). Additional factors pertaining to the variability of material properties of the participating components (mainly those of cement and the formation) further complicate the interpretation of the field results. If such variations due to material properties as well as interface conditions are smooth, interpretation of CBL results is usually not a difficult task. In practice, however, there several uncertainties caused by all factors discussed above. Especially, CBL measurements have been found sensitive to the water-filled microannuli (Jutten et al., 1993). Some of the key drawbacks of sonic tools will be discussed later on in this report by comparison to ultrasonic tools (see Section 6.3).

6.2.2 Ultrasonic Tools

In the early eighties, in an effort to improve acoustic logging methods, Schlumberger Inc. presented a new generation of logging tools (Froelich et al., 1982) called CET (Cement Evaluation Tool). The latter is a high-frequency ultrasonic tool. Similarly, Halliburton Logging Services developed another ultrasonic tool (Sheives et al., 1986) called PET (Pulse Echo Tool). Both tools were developed in order to overcome some of the drawbacks of the conventional sonic techniques such as CBL. In both CET and PET, the basic configuration consists of several focused transducers arranged in a helical pattern (double helical pattern in the PET case). By employing several transducers in the azimuthal direction, the response and consequently the distribution of the parameter of interest around the casing can be obtained. These transducers emit a short pulse of acoustic energy and then receive the echo from the casing.

In the CET, the eight transducers are positioned in a helical pattern on the sonde at 45° from each other. The ultrasonic transducers have approximately one inch diameter and they act both as emitters as well as receivers. A ninth transducer is set in the axial direction in order to monitor wavespeeds in the fluid. General configurations of CETs are illustrated in Fig. 7(a) for two different mandrels: 3-3/8" diameter (for casings from 4-1/2" to 5-1/2") and 4" diameter (for casings from 5-

1/2" to 9-5/8"). The log is divided into three tracks: left, right and middle track. As seen in Fig. 21, two sets of centralizers are provided to support the sonde body. Transducer eccentering effects result in a non-vertical incidence of the ultrasonic beam. Accordingly, the beam is reflected away from the transducer.

Fig. 21(b) depicts some of the fundamental principles underlying the ultrasonic measurements. As indicated above, the transducers have a dual function: they are both sources as well as receivers. They are positioned at approximately 2" from the casing wall. A short ultrasonic pulse is sent towards the casing. After traveling through the mud or fluid, some of the pulse is reflected right back from the frond face of the casing wall. As shown in Fig. 21(b), the refracted pulse enters the casing wall and consequently is reflected back and forth at both faces with some of the pulses refracted again and therefore transmitted outside the thickness of the wall. The objective is to cause the casing wall to resonate in its thickness mode.

The reflection of the ultrasonic signal depends on the acoustic impedances of the casing and those of the materials in contact with it (water or mud on one side and the formation on the other). With regards to the frequency of the ultrasonic pulse, the casing wall thickness appears to be a determining factor for the casing impulse response. The wall thickness ranges from 0.2" to 0.6". In order to resonate the casing in its fundamental mode, the ultrasonic pulses must have a frequency bandwidth from 600 kHz to 300 kHz. Impulse responses from a free and cemented pipe are shown in Fig. 21(b). They are presented by a sequence of pulses separated by twice the travel time through the casing wall. The difference between these two cases is reflected by the rate of signal attenuation with the case of cemented pipe attenuated more quickly than that of the free pipe. In general, the presence of the good cement is signified by damping out the resonance faster than poor cement.

The PET uses also eight ultrasonic transducers, but they are arranged along the sonde in a double helical array pattern (see Fig. 22a). They also employ a ninth transducer to evaluate fluid travel time. The PET measurement principle is shown in Fig. 22(b). Free-casing and cemented-casing response signals are also depicted. The PET response signals can be converted to compressive strength representations by employing relationships between compressive strength versus acoustic impedance.

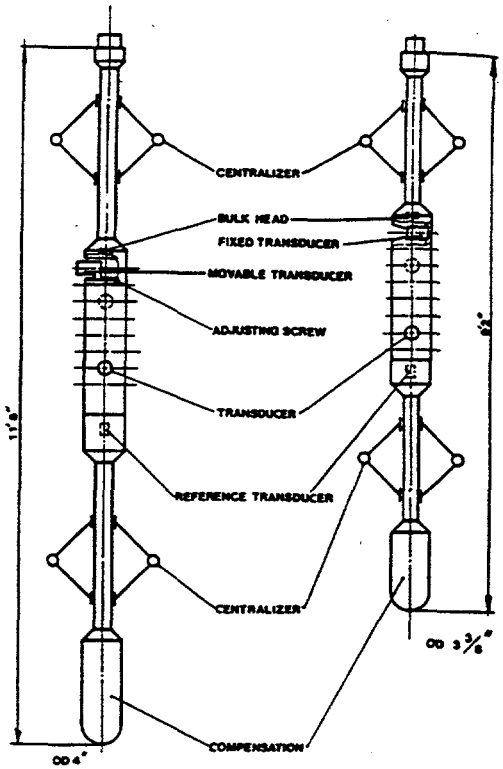

(a)

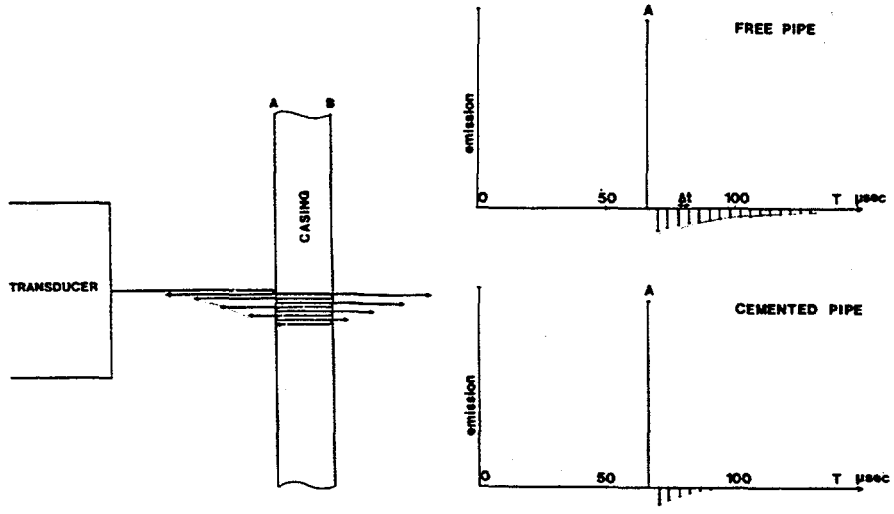

(b)

Figure 21. Cement Evaluation Tool: (a) Tool, (b) Principle of Measurement (after Froelich et al., 1982).

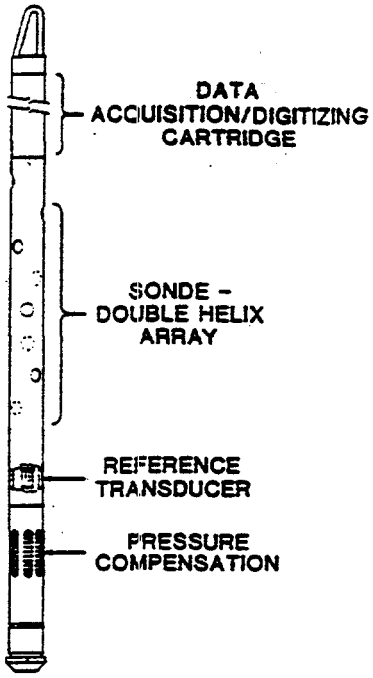

(a)

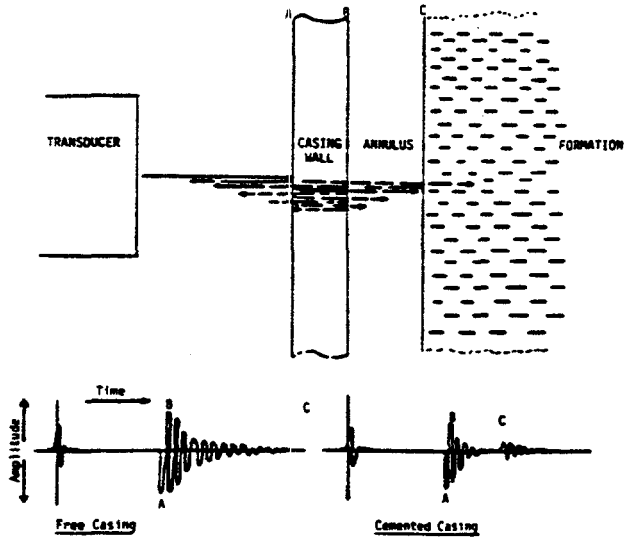

(b)

Figure 22. Pulse Echo Tool: (a)Tool, (b) Principle of Measurement (after Albert et al., 1988).

6.3 Application to GHP Field Evaluation

Experience from field measurements has led to the conclusion that there are several advantages and disadvantages associated with both sonic and ultrasonic methods. As indicated previously (Section 6.2.1), the omnidirectional character of the transmitter and receiver in sonic measurements is a key disadvantage. First, it requires good tool centralization in order to obtain simultaneous arrivals from all directions. Second, the method is characterized by lack of azimuthal resolution. Therefore, it neglects material and bonding distributions around the pipe. Azimuthal averages usually provide misleading results. By contrast, the major advantage of the ultrasonic techniques is that it provides such spatial resolution.

As described in Section 6.2.1, shear coupling is important for the sonic technique. Lack of shear coupling is caused by the presence of microannuli. Therefore, a second major disadvantage of the sonic techniques is their sensitivity to microannulus effects (Jutten et al., 1993). On the other hand, ultrasonic techniques are not sensitive to shear coupling. They operate by pulses generated to strike the wall surface at normal incidence. When sensitivity to shear coupling, however, is important, then sonic techniques are more efficient than ultrasonic ones. Experimental results from comparisons between the two techniques in a full-scale simulator, have lead to the conclusion that combinations of sonic/ultrasonic measurements should be used in field verification programs (Hayman et al., 1995).

Another important conclusion reached after several years of experience by the petroleum industry, is that the progress made in this area since the appearance of earlier techniques (around fifties) is not significant. Even with the latest technology, it appears that the existence of gaps formed at the cement-formation interface cannot be measured. Therefore, unless a channel is in contact with the casing (see Fig. 6d), its existence is not detected. As it was pointed out in Section 6.1, the integrity of the cement/formation interface is very significant also from environmental considerations. Channeling facilitates transport of contaminants and it is more detrimental in this regard as compared to material permeability fluctuations. Pulsed Neutron Logging (PNL) has also been used for channel detection (see e.g., Sommer et al., 1993). PNL measures the rate of capture of thermal neutrons by the various components of the system.

Additional evidence for using a dual approach (i.e., sonic/ultrasonic) was obtained in an investigation conducted by the EPA (Albert et al., 1988). The objective of that investigation was to establish guidelines for what is called mechanical integrity verification. Specifically, EPA regulations require that all Class II injection wells have to demonstrate mechanical integrity before operations begin and at least once every five years thereafter. A test well was constructed and various service companies were invited to use their tools for evaluating cement bond at the cement/casing as well as cement/formation interfaces. Low frequency (20 kHz) as well as high frequency (500 kHz) techniques corresponding to the two basic generations of logging tools were applied in a test well constructed with intentional imperfections. While several successful measurements were made, the conclusion by Albert et al., is that none of the tools used in the EPA

study was able to detect channeling in the cement smaller than 30 degrees. Cement channeling of the latter size is considered environmentally unacceptable.

The consensus in the geothermal pump industry is that in order to demonstrate confidence with GHP ground heat exchangers, field tests are highly important. Currently available technology of sonic/ultrasonic measurements can be used to evaluate the in-situ condition of the bonding at the backfill-pipe as well as backfill-formation interfaces. One of the apparent anticipated difficulties is the size of the tools, since the diameter of the pipe in the ground heat exchanger is much smaller than that of injection or production wells (standard CBL measurements are made in wells with inside diameter of two inches or larger). Discussions with Halliburton indicated that the smallest CBL tool available has a diameter of 1 11/16". This is somewhat larger than the internal diameter of HDPE pipe typically used for GHP heat exchangers. Halliburton suggested that a CAST-V (ultrasonic) tool would be better at detecting the presence of grout than a CBL tool. However, a small diameter CAST-V tool is not available. If the geometry limitations can be overcome, both sonic and ultrasonic techniques can provide information on the backfill/pipe interface conditions and, by following historic experience from petroleum industry, they should be used in combination.

An additional complicating factor arises from the nonsymmetrical configuration of the GHP heat exchangers created by the presence of two pipes. This causes an unequal azimuthal distribution of the grout or other backfill material around each of the pipes. Any arrival times from waves reflected at the backfill/formation interface they are inherently unequal. In addition, pipe-to-pipe effects may be of importance when resonance is caused in one pipe. On the other hand, the existence of the second pipe can be used to perform crosshole type measurements. In this case, appropriate engineering analysis should be made to determine what are the measurable quantities and at what frequency range they apply. Sonic and ultrasonic measurements must be calibrated to take into account the polyethylene pipe vibrations which differ from those of steel pipe as well as backfill dynamic material properties. The wavespeeds of acoustic waves in some of the non-cement type grouts used as backfill (i.e., bentonite backfills) can be significantly different than those of cement-based grouts. Engineering calculations, on the basis of the acoustic impedances of representative backfill materials, must be made to further evaluate the applicability of acoustic methods in determining the in-situ integrity of ground heat exchangers of GHP systems. Wandering (lack of centralization) of the U-loop within the borehole also needs to be taken into consideration for techniques involving insertion of a probe into a leg of the U-loop. Finally, as it will be discussed in Section 6.5 of this report, forced vibration techniques should complement the acoustic methods of field evaluation.

6.4 Other NDT Methods

Generally speaking, we advocate acoustic methods in combination with forced vibration techniques to be the main focus of the field verification of GHPs heat exchanger systems. It is instructive, however, to acknowledge some other relevant NDT methods. For example, temperature logs can be used with cement grouts while the grout still generates heat in the exothermic stage.

Gamma-gamma density logs are used to evaluate backfill materials. Furthermore, a variety of methods are available for detecting vertical leakage in the annular space between the pipe and the formation. Some of them are based on temperature logs which can detect very low rate leakage. Similarly, radial differential temperature logs (RDT) are used for this purpose. Temperature is measured at two points 180 degrees apart. Temperature differences are indicative of flow of cooler water. Finally, radioactive trace-ejector has been used to trace flows in the annular space between the casing and formation by the petroleum industry.

A variety of additional measuring techniques are also available for verification of in-situ conditions in addition to acoustic and thermal methods. Magnetic and electrical methods as well as radiography have been used for verification purposes. Such methods are well accepted NDTs especially for steel structures and general ferromagnetic materials. More recent techniques include sonar and impulse radar. The latter measures differences in dielectric material constants based on which material flaws are detected. Seismic methods, however, appear to be more suitable for application to ground heat exchangers. Seismic tomograms such as crosshole tomography has been used in the detection of underground structures (see e.g., Su and Cotten, 1992). However, tomographic surveys have to be carefully planned so that they become sensitive to the conditions at the borehole interface. Crosshole seismic testing have been used as NDT method for remote testing of grouted radioactive wastes as part of a quality verification program (Benny and Olson, 1991). A set of source-receiver configurations was placed inside the grouted waste through 2" PVC pipes. Again, seismic methods need to be adequately studied before suggesting further consideration for application to GHPs.

Crosshole seismic testing has the advantage of placing the seismic source exterior to the ground heat exchanger. As mentioned previously, sectional limitations of the latter pose restrictions with regard to instrument dimensions that can be lowered within the pipes. A systematic analysis is required, however, to determine the amount and location of receiver boreholes in relation to the heat exchanger. Furthermore, appropriate studies must be made to evaluate the type of response to be measured and how it relates to the backfill/formation interface conditions, which is targeted by the field measurements.

Finally, some of the wave propagation methods used in verification activities of pile foundations should be given special consideration. They appear to have close resemblance to the ground heat exchangers although their respective functions are completely different. Historically, pulse-echo sonic methods have been used to perform nondestructive tests on concrete piles.

6.5 Low Vibration Methods

The seismic methods discussed in the previous section have a common characteristic, in that, the seismic source is placed away from the object of interest. Specifically, it is placed within the source borehole at some prescribed depth. Seismic waves are reflected and refracted after they impinge on the backfill and some of them are captured by the various receivers. The importance of

the paths traveled by the various waves generated by the seismic source, is that, it can be ultimately related to specific information about the condition of the materials encountered as well as the continuity of the medium. In this section we are suggesting the use of an opposite approach to what was just described. Specifically, the source is placed on the ground heat exchanger. This concept has been used extensively in the domain of vibration of foundations.

The proposed test procedure for GHPs is as follows:

A vibration transducer is placed at the top of the ground heat exchanger and causes it to vibrate in a specific mode, e.g., vertical motion. The vibration of the ground heat exchanger produces a set of waves that radiate away from it into the surrounding formation. These waves consist primarily of body waves, surface waves as well as interface waves depending on the stratigraphy of the formation. The motion is recorded at the top of the ground heat exchanger. Other locations may also be selected to provide additional response data. The force-displacement relationship for the particular mode of vibration excited during the test is recorded. The latter is conventionally presented in terms impedance or compliance functions over a dimensionless frequency range which usually represent ratios of wavelengths to some dimension of interest, i.e., radius or height.

Theoretically, the ability of the ground heat exchanger to radiate energy away into the formation depends, among other factors, on the interface conditions between the backfill and the formation. The better the bonding the more the radiated energy. This principle can be translated in terms of impedances. Specifically, loss of bonding due to the presence of channeling in the backfill would influence the appearance of these curves in specific frequency windows. Therefore, by comparing to a full-bonding curve conclusions can be drawn with respect to backfill/formation interface. Specific ranges can be developed from laboratory testing where specimens can be subjected to vibratory motion. By recording their dynamic response, field specifications can be developed. Furthermore, dynamic analysis of the overall system should be performed using finite element techniques to calibrate these tests.

Vibration tests require knowledge of the properties of the formation. Such properties are defined with better confidence when obtained by geophysical tests. Laboratory tests such as resonance column tests can supplement the definition of site properties. Preferably, geophysical investigations of the site should be performed. Material properties of the formation should be defined in terms of depth. Vertical profiles of shear wave velocity, material damping and density are required.

The rigidity of the ground heat exchanger is another parameter of investigation since it is directly related to the properties of the backfill material. If the vibrations result in sufficient relative deformations in the backfill, then the response waveforms should contain information about the properties of the backfill material. This can be used to evaluate if the quality of the backfill i.e., if it is competent or if it has been mixed with formation material during the construction process or

otherwise varies from design specification. Again, using vibration techniques to check on the in-situ condition of the backfill material requires that the backfill be excited and respective stress waves are generated along the heat exchanger. The magnitude of these effects is difficult to judge without performing relevant analytical studies. Similarly, it would be rather difficult to predict if vibration methods can be used to evaluate the bonding condition at the pipe-backfill interface. Such effects are probably of secondary nature. This is because the system rigidity is primarily dominated by that of the backfill material. Thus, it would be more appropriate to tackle the pipe/backfill in-situ bonding verification with combination of sonic and ultrasonic methods.

7.0 NUMERICAL MODELING OF HEAT TRANSFER

BNL is developing necessary numerical models to study the response behavior of the ground heat exchangers employed by the GHP. The objectives of this task are twofold:

1. to establish benchmark problems for evaluating system behavior, and
2. to support field testing and required interpretation of test results.

Currently, two types of engineering analysis are considered: (a) heat transfer, and (b) dynamic response respectively. A general description of the heat transfer problem and a review of currently available methodologies are given in Section 7.1. Preliminary results from finite element analysis are presented in Section 7.2. Dynamic response evaluations with additional heat transfer analysis of GHP ground heat exchangers will be reported in the future.

7.1 Current Methodologies

The heat transfer problem related to ground heat exchangers has been studied both analytically as well as experimentally. Among others, most recent studies are those by Gu and O'Neal, 1998 and Rottmayer et al., 1997. Both studies recognize the difficulties of the problem and offer some solution approaches. The latter are still limited by several factors i.e., those required to model interface conditions, horizontal or vertical nonhomogeneous formations and, in general, true three-dimensional effects. Much additional computational and modeling work needs to be done so that more realistic conditions met in practice can be modeled.

As indicated by Rottmayer et al., 1997, most available analytical studies employ classical solutions for the line source problem (Ingersoll et al., 1954) or for the cylindrical source problem (Carslaw and Jaeger, 1946). Accordingly, a finite difference approach was proposed considering approximate three-dimensional transient conductive heat transfer analysis. In order to account for noncircular geometry representation of the pipes within the borehole, a geometric factor was introduced so that circular pipes are approximated by noncircular sections. The validity of this assumption was explored by numerical simulations. Furthermore, the model is based on heat transfer within horizontal planes. It is therefore assumed that heat transfer takes place in axial and circumferential direction. No axial conduction is allowed.

The resistance network for a cylindrical mesh was developed by Rottmayer et al., 1997 using logarithmic distance relation for radial resistance as dictated by line source Green's function solution. Modeling was based on a ground storage volume which is defined as a cylinder height equal to the depth of the borehole and radius equal to the far-field radius. Discretization vertically considers slices of the ground storage volume while axially it is divided into several sections. Thus, at a given depth a specific cylindrical finite-difference grid is associated with the model. Solution times for annual simulation were drastically reduced by splitting the solution time by time steps required for the fluid transport and the heat transfer to the ground.

It must be recognized that the ground heat exchangers of the GHP configuration impose two fundamental challenges to the analysis and modeling of the heat transfer problem. The first arises due to the non-symmetric geometry while the second is due to the non-symmetric thermal loading condition. The presence of the two pipes in the U-tube instead of one eliminates the use of axisymmetric field analysis. On the other hand, fluid temperatures in the two pipe legs are generally different thus introducing a non-symmetric loading condition. If, additionally, one considers variations in formation surrounding the heat exchanger, then true three-dimensional solutions are required to tackle this heat transfer problem.

Due to these physical complexities of the system, a complete 3D analytic solution is very difficult to obtain and thus several simplifying solutions have been used. It is often assumed that the medium associated with the heat exchanger configuration is homogeneous for the purpose of studying GHPs in the cooling mode. This would be a reasonable assumption provided that the properties of the formation and those of the backfill are very close. If not, such approach will generally produce erroneous results.

Furthermore, Gu and O'Neal, 1995 developed an analytic solution of the case of a cylindrical heat source in a nonhomogeneous medium by taking into account that the backfill and the surrounding formation have different properties. Such solution allowed evaluations of the effect of the backfill on the transient heat transfer considering different site conditions. Using the solution for a single cylindrical source, Gu and O'Neal, 1998 developed an approximate equivalent diameter solution for the U-tubes using steady heat conduction and superposition techniques. This approach seems very attractive since it eliminates the need for considering the two pipes of the U-tube. Concerns related to thermal short circuiting (thermal interference) between the two pipes are incorporated in the derivation of the equivalent diameter. The ranges of validity of the equivalent diameter, however, should continue to be investigated.

In the preceding discussion we presented some of the latest modeling techniques and pertinent solutions to the heat transfer problem encountered in GHP heat exchangers. Comparable techniques have been used in other similar studies (e.g., Couvillion and Cotton, 1990). We conclude that the majority of the available approaches make use of conventional source solutions for the point, line or plane source in an infinite medium. An analytic effort was made to develop solutions that

incorporate nonhomogeneous conditions arising from the presence of the formation. Discretization is typically performed through finite-difference. Application of the finite element method (FEM) to treat this problem appears to be practically nonexistent on the basis of our limited review. Computer modeling work is fundamentally of the finite-difference type.

The above briefly reflect the trend of the current state-of-the-art modeling of the heat transfer problem in GHP heat exchangers. Until general three-dimensional solutions are developed, such approximate modeling approaches should be used on a case-by-case basis. In addition, a frequent application of finite element techniques should be considered by the geothermal pump industry to tackle more realistic situations encountered in practice.

7.2 FEM Analysis

Current numerical modeling performed at BNL for the GHP program is based on the finite element technique. Two type of analyses are considered, namely,

1. heat transfer analysis
2. dynamic response analysis

Plane and axisymmetric two-dimensional (2D) models are first analyzed. During the next phase of the program, three-dimensional (3D) models will be constructed so that 2D vs. 3D comparisons can be made. Preliminary results have been obtained from 2D models and samples are presented in this section of the report.

A set of 2D models was developed that incorporate all components of the ground heat exchanger: pipe-backfill-formation. The latter components have been all discretized into a medium size FE mesh which is shown in Fig. 23. In this example the radius of soil was set at 2.5 times the radius of the grout. (i.e., $r_{soil}=2.5r_{grout}$). This modeling was preceded by a more coarse mesh used to initialize the modeling process. A finer mesh would yield more detailed results. However, through comparative computer runs, it was determined that the current model gives reasonable accuracy for the response quantities of interest.

The sectional configuration of the GHP heat exchanger with U-tubes would permit the use of planes of symmetry to reduce the model size. There were, however, specific reasons for employing full (360°) 2D models. The primary reason is to allow simulation of non-symmetric interface conditions either at the backfill-pipe or at the backfill-formation interfaces. Due to their inherent assumptions, none of the available latest modeling approaches discussed in Section 7.1 would be able to treat such boundary conditions, both in terms of spatial variation as well as in terms of the type of continuity enforced at the boundary.

The particular interface conditions considered are: (a) for the heat transfer problems: modeling of arbitrary development of microannuli at the pipe/backfill interface, and (b) for the

dynamic analysis problems: allow gaps to form at the backfill/formation interface. Such engineering evaluations are expected to quantify a variety of concerns related to the performance of GHP systems. Typical results obtained from 2D finite element solutions of the heat transfer problem in GHP systems are shown in Fig. 24. Specifically, Figs. 24(a) and (b) display temperature distributions obtained from two solution cases, namely, operation of the pump in cooling and heating modes, respectively. The corresponding entering and leaving waters temperatures (EWT & LWT) for the latter two modes of operation were:

MODE	EWT (°F)	LWT (°F)
Heating	35	41
Cooling	86	96.8

Finally, the far-field temperature was taken to be 55.4 °F. It is recognized that the far-field radius under operating conditions may be greater than that used in the preliminary examples presented. This is particularly the case after several years of operation when storage effects become significant. Future work will examine this aspect in more detail, along with the impact of interfacial conditions on heat transfer. Knowledge of the temperature distribution throughout the grout will be used to analyze other aspects of behavior such as stresses induced by thermal expansion.

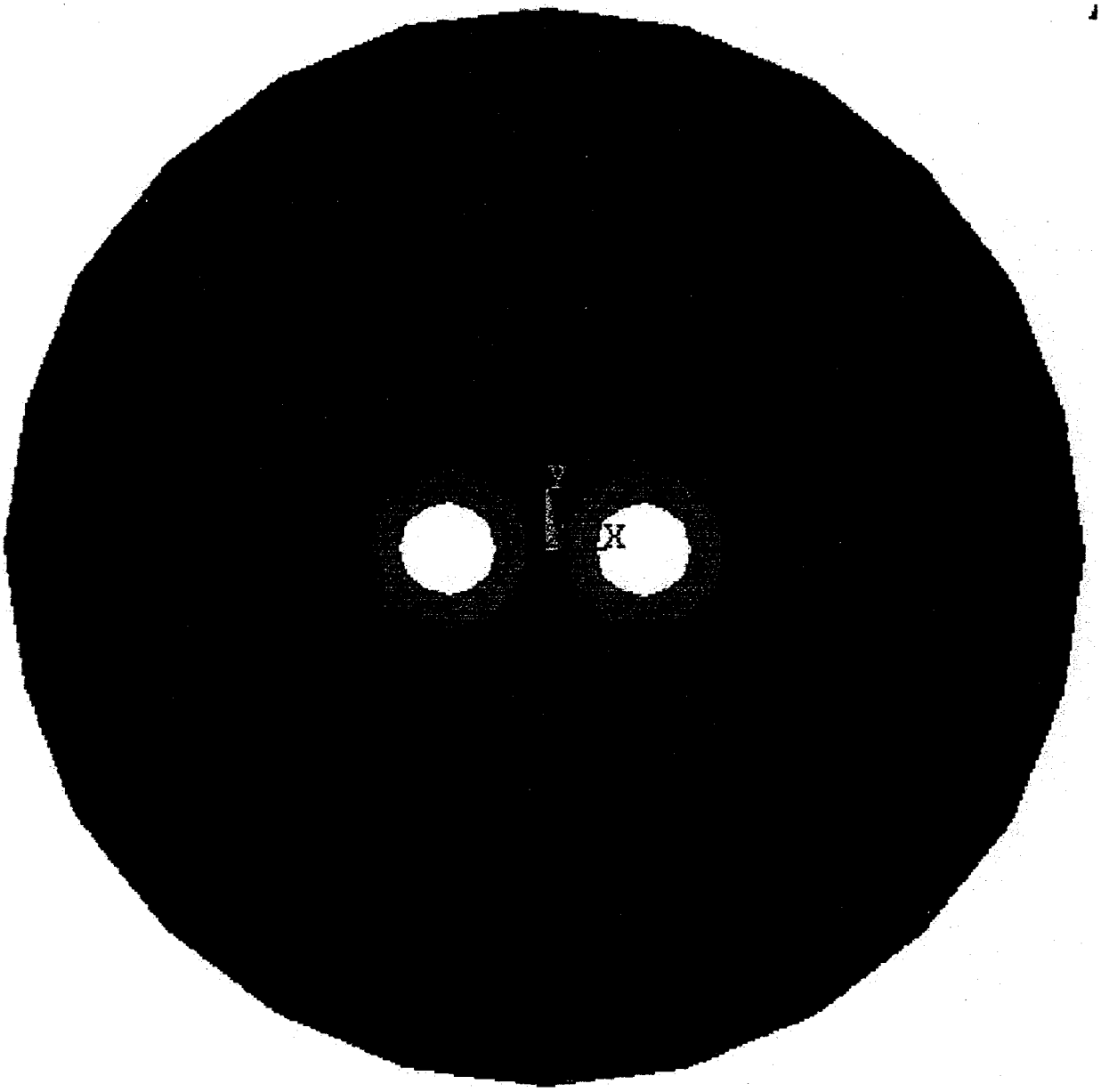

Figure 23. Two Dimensional Finite Element Model of GHP Heat Exchanger.

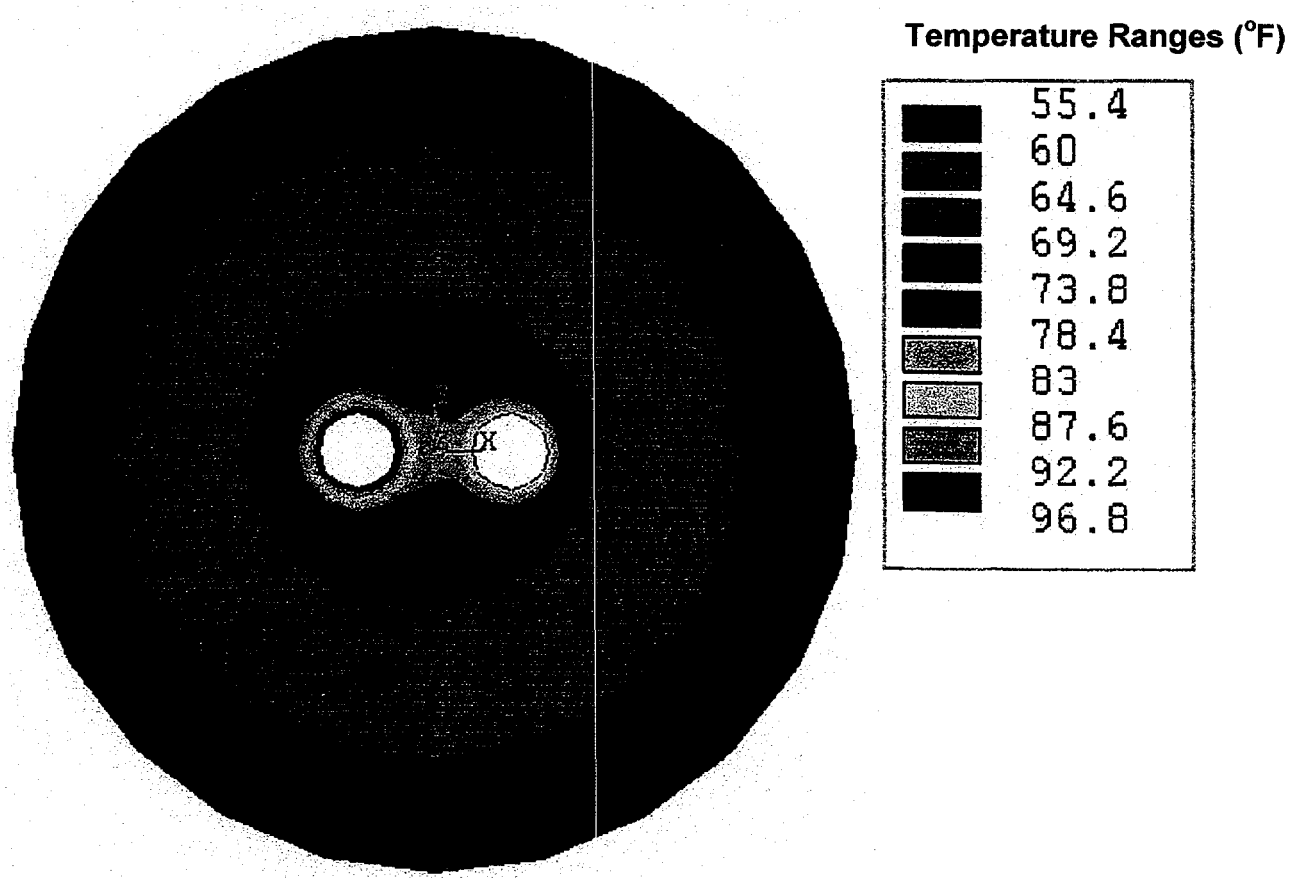

Figure 24a. Heat Transfer Analysis: Cooling Mode

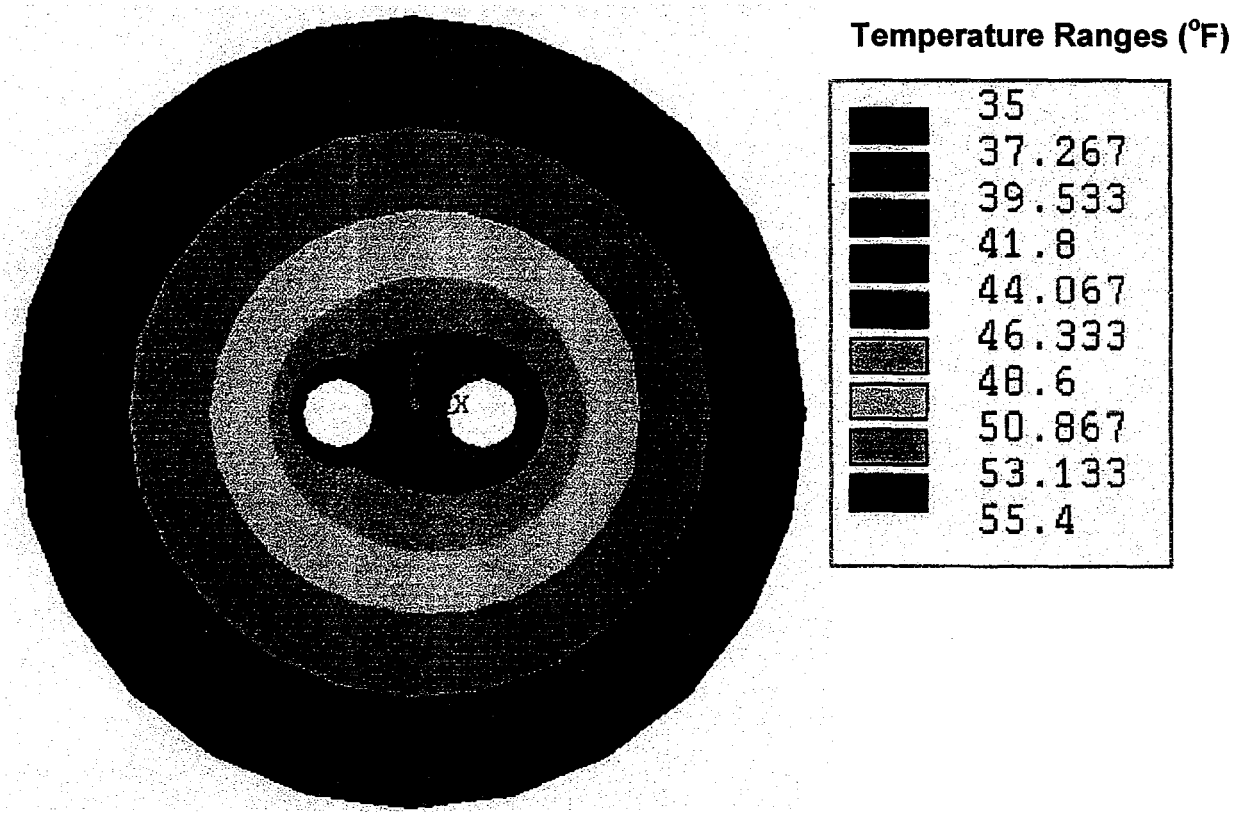

Figure 24b. Heat Transfer Analysis: Heating Mode

8.0 SPECIFICATIONS FOR THERMALLY CONDUCTIVE CEMENTITIOUS GROUT

8.1 Materials

8.11 Cement

The cement used shall conform to ASTM C 150-Type I. If the site conditions require that sulfate resistant cement is necessary then Type II or Type V cement can be used. It is possible to partially substitute fly ash or ground granulated blast furnace slag for cement. However, this changes the rheological, shrinkage and bonding characteristics of the grout (Allan, 1997). Cement that already contains a waterproofing additive should not be used as this has been found to cause slight foaming of the grout and reduce the thermal conductivity.

Cement should be kept dry at all times, stored on pallets and covered with a tarpaulin or plastic sheet. Any bags of cement that are damaged (e.g., torn) or that have been exposed to water should be discarded. The cement should be fresh and free from any hard lumps.

8.12 Bentonite

The decision to use to bentonite will depend on the mixing equipment used. For low shear (e.g., paddle) mixers it may be necessary to use a small amount of bentonite to aid grout stability and reduce segregation of sand. The bentonite used shall be 200-mesh sodium montmorillonite. The viscosity of the grout will increase with increasing proportion of bentonite.

8.13 Water

The mixing water shall be potable. Water with excessive impurities may affect the final properties of the grout.

8.14 Silica Sand

The silica sand shall conform to ASTM C 33 in terms of soundness and absence of deleterious substances. The particle size gradation shall conform to that in Table 19 below. Other sand gradations would probably require changes in water/cement ratio and superplasticizer dosage to make the grout pumpable and these changes would affect the final properties of the grout. The sand used in this work was purchased from New Jersey Pulverizing Co. (Test Card 3343-97). However, sand suppliers in other states should be able to blend sand to meet the specified gradation.

The bags of sand should be kept dry at all times and stored on a pallet. Sand that has become wet should not be used as this will increase the water/cement ratio of the grout.

Table 19. Specification for Particle Size Gradation of Silica Sand

Sieve No. (Size, μm)	Percentage Passing (%)
8 (3350)	100
16 (1180)	95-100
30 (595)	55-80
50 (297)	30-55
100 (149)	10-30
200 (75)	0-10

8.15 Superplasticizer

The superplasticizer shall be ~42% sodium naphthalene sulfonate conforming to ASTM C 494 Type F. The product used in this work was Rheobuild 1000 from Master Builders Technologies. Other manufacturers supply equivalent products. Superplasticizer can often be obtained from local concrete ready mixed companies.

8.16 Equipment

The bentonite should be premixed with water preferably in a high shear mixer. It is difficult to achieve uniform distribution of bentonite in a paddle mixer. The grout can be mixed in either a low shear (paddle) or high shear (colloidal) grout mixer. Paddle mixers are less expensive than colloidal mixers, but also less effective and require greater mixing time. Discharge from the mixing tank to the pump hopper is by gravity and, hence, is slower. Improved sand carrying capacity, decreased water requirement, reduced bleeding and greater flowability of grouts is usually achieved with grouts mixed in colloidal mixers. Colloidal mixers improve wetting of the cement and sand particles and prevent segregation.

It is preferable to use a grout mixer in conjunction with a larger capacity agitator in which the grout is stored and agitated until use. This is necessary to keep the particles in suspension, and, in the case of thixotropic grouts, keep the grout mobile and fluid. As discussed previously, the grout can be pumped continuously from the agitator tank while the next batch is mixed. Thus, pumping is not interrupted and the risk of plugging the tremie tube is reduced. Colloidal mixers are available in a range of capacities (typically 60-127 gallons), including trailer-mounted units. It is critical that

a proper grout mixer suited to cement-sand grouts be used. Mixing of the grout by hand, pumps or concrete ready mix trucks is not acceptable.

Piston pumps are recommended for pumping the cement-sand grouts. Excessive wear may be encountered when using a helical rotor (progressing cavity/Moyno) pump. Based on the field trials a minimum 1.25-inch diameter tremie tube with an open end and several side discharge outlets is recommended. The tremie tube should be cleared with water prior to grouting to remove any material introduced during insertion into the borehole that may plug the outlets.

8.3 Grout Mixing Procedure

Depending on the mixing equipment and actual particle size gradation of sand used, some variation in the mix proportions may be necessary. Irrespective of the mixer used, it is recommended that trial mixes are performed and water or superplasticizer adjusted so that suitable pumpability is achieved. Trial mixes will also determine whether it is necessary to use bentonite in the grout to prevent sand segregation. However, use of excessive water will be detrimental to the hardened grout properties (e.g., shrinkage, permeability, durability, thermal conductivity) and probably induce segregation of the sand. Excessive superplasticizer will increase shrinkage and should be limited to a maximum of 20 ml/kg cement. This is equivalent to 851 ml per 94 lb. bag of cement.

The basic mix is given in Table 5. The amount of grout that can be mixed at once will depend on the capacity of the grout mixer. It is preferable to mix as much as possible per batch.

Since the grout properties are very sensitive to w/c and superplasticizer dosage, it is critical that the amounts of water and superplasticizer required for a grout batch are measured accurately. This can be achieved through use of graduated containers or, in the case of water, with a water meter.

Table 5. Mix Proportions and Yield for Batch of Mix 111 Based on One Bag of Cement.

Cement	1 x 94 lb. bag
Water	23.5 litres (6.19 U.S. gallons)
Sand (conforming to spec.)	2 x 100 lb. bags
Superplasticizer	639 ml (1.35 pints) (approximately, not to exceed 851 ml)
Bentonite (optional)	470 g (approximately)
Yield	72.2 litres (19.1 U.S. gallons)

The recommended procedure for mixing the cement-sand grout is as follows:

1. Pre-mix bentonite with the required, measured quantity of water in a high shear mixer until bentonite is uniformly dispersed. (A Jiffy mixer may suffice).
2. Place water-bentonite mix in grout mixer.
3. Place required measured quantity of liquid superplasticizer in mixer.
4. Start mixer at low speed.
5. Mix water and superplasticizer for approximately 10 seconds. Care should be to avoid air entrainment by mixing at excessively high speed.
6. Gradually add required quantity of cement in mixer and increase mixer speed. Mix for approximately one to two minutes or until cement is well dispersed.
7. Gradually add required quantity of sand in mixer and increase mixer speed if necessary.
8. Mix grout for specified time (Maximum of 5 minutes should be adequate).
9. Transfer grout to agitator. If agitator is not used then transfer grout to hopper. Grout in hopper should be agitated occasionally with Jiffy mixer or similar.

At the conclusion of the grouting all equipment should be thoroughly washed with water. Equipment should be used and maintained according to manufacturer's guidelines.

8.4 Quality Control

Every batch of freshly mixed grout should be measured for specific gravity prior to pumping. This requires use of a mud balance available from companies such as Baroid and the test procedure is given in ASTM D 854-83. The specific gravity is sensitive to water/cement ratio, sand/cement ratio and uniformity of mixing. Mix 111 with the proportions given above has a specific gravity of 2.18 (Density = 18.2 lb./gal). As a guide, the specific gravity should be 2.18 ± 0.02. Measuring flow time in accordance with ASTM C 939 can also be performed to check for grout pumpability and uniformity. All data and any changes in grout mix proportions or mixing procedure should be documented by the grouting contractor.

Samples should also be taken for future laboratory thermal conductivity testing. In this case, the grout should be poured into a suitable leakproof mould, the dimensions of which depend on the equipment that will be used to measure thermal conductivity. The grout samples should be sealed or covered with plastic for 24 hours and maintained at temperature as close as possible to 20-25°C. After 24 hours the samples should be demoulded and immersed in a water bath at 20-25°C to cure for at least 7 days prior to testing.

9.0 FUTURE WORK

In FY 99 it is planned to perform the following:

- Continue monitoring long-term performance of grouts used in FY 98 field trials.
- Conduct in-situ permeability tests and numerical modelling of seepage in grouted boreholes.
- Develop, analyze and demonstrate non-destructive test method for verification of bond integrity and quality control in grouted boreholes.
- Determine effect of contact resistance on heat transfer.
- Provide technical assistance to commercial users of thermally conductive cement-sand grouts.

10.0 CONCLUSIONS AND RECOMMENDATIONS

A relatively simple and economic thermally conductive cementitious grout has been developed, characterized and field demonstrated. Cement-sand grouts have significantly higher thermal conductivity than neat cement and bentonitic grouts and show better retention of conductivity under drying conditions. The thermal conductivity of the optimum grout (Mix 111, a.k.a. Bonus Grout) was 2.42 W/m.K (1.40 Btu/hr.ft.°F) when wet cured. This compares with 0.80 to 0.87 W/m.K (0.46 to 0.50 Btu/hr.ft.°F) for neat cement grout, 0.75 to 0.80 W/m.K (0.43 to 0.46 Btu/hr.ft.°F) for conventional high solids bentonite grout and 1.46 W/m.K (0.85 Btu/hr.ft.°F) for thermally enhanced bentonite. The increased thermal conductivity results in potential reduction in required bore length for geothermal heat pumps and, hence, decreased installation costs. Potential bore length reductions may be up to 22 to 37% based on calculations performed in FY 97 and depending on bore diameter, soil type and other variables. Furthermore, the cement-sand grout has other benefits as compared to alternative grouting materials. These include enhanced bonding to U-loop, low permeability, low shrinkage, mechanical strength and durability under wet-dry and thermal cycles.

Field demonstrations showed that the grout (Mix 111/Bonus Grout) could be mixed with a conventional paddle mixer and pumped using a piston pump. Addition of a small quantity of bentonite improved grout stability and reduced the tendency of sand to settle. It is recommended that a mixer/agitator plant be used in which the grout is continuously agitated as it is pumped while a new batch of grout is mixed. The four boreholes that were grouted with Mix 111 will continue to be monitored for heat transfer behaviour. Specifications for materials, mixing and placement of the grout as outlined in this report should be followed to achieve the required thermal properties, impermeability and durability. It would also be feasible to prepackage the dry ingredients although this will increase cost.

Extensive coefficient of permeability (hydraulic conductivity) testing over a representative range of temperatures and feasibility analysis of potential non-destructive test methods were performed to address concerns raised by environmental regulators regarding the hydraulic sealing capability of GHP grouts. The permeability results showed that Mix 111 cement-sand grout has superior bonding and sealing characteristics compared to neat cements. The improved bonding will also enhance heat transfer. The laboratory permeability tests involved testing the specimens under constant temperature conditions. Thermal gradients due to different temperatures in loop legs were not simulated. Therefore, in-situ permeability tests on grouted boreholes are recommended to confirm the suitability of the grout under operational loads.

Field verification is required to ensure that sufficient bonding exists between grout-loop and grout-formation under operating conditions. This could be achieved through in-situ permeability and in-situ non-destructive tests. For the latter, two approaches are recommended. First, a combination of sonic/ultrasonic measurements should be considered. Experience from field tests and related verification studies performed by the petroleum industry suggests that using one of these techniques alone can lead to unacceptable results in the sense that actual field conditions can be completely misrepresented. Therefore, these two techniques should be used in combination. An apparent difficulty of using sonic and ultrasonic measurements is related to the narrowness of the diameters of the polyethylene pipes used to construct the ground heat exchangers. Furthermore, the nonsymmetrical cross section of the ground heat exchanger and potential lack of centralization is expected to cause uneven distribution of the response waveforms in azimuthal direction. Similarly, the flexibility and damping characteristics of the polyethylene pipe needs to be taken into account since such measurements have typically been performed in liquid filled wells with steel casing. Effects from these deviations must be considered in sonic and ultrasonic measurements.

Second, a set of low level vibration tests should be designed for field verification of ground heat exchangers to complement sonic/ultrasonic measurements. Vibration transducers can excite the heat exchangers in certain modes of vibration. The motion can be recorded at the top and the measurement can be put into the form of force-displacement relation (compliance function). Comparisons with those of a fully bonded case would lead to respective bonding evaluations.

From a review of the state-of-the-art modeling approaches used in available heat transfer evaluations we concluded that several limitations exist. Specifically, there are several difficulties associated with the development of analytical approaches required to model the behavior of ground heat exchangers and surrounding media. Primarily, they arise due to lack of symmetry in geometry and loading condition. Thus, most available analytical models are based on classical solutions for the line or cylindrical source problem in uniform media. Because of their inherent limitations, such models cannot adequately describe actual field conditions. Accordingly, we believe that there is a need to perform finite element modeling and analysis of the response behavior of ground heat exchangers. Such an approach is expected to complement those of existing studies. Finite element analysis is highly justifiable in situations where more realistic representations are desired in order to reflect actual field conditions.

11.0 REFERENCES

ACI 304.1R, Guide for the Use of Preplaced Aggregate Concrete for Structural and Mass Concrete Applications, American Concrete Institute Materials Journal, V. 88, No. 6, pp. 650-668, 1991.

Albert, L.E., Standley, T.E, Telo, L.N., Alford, G. T., A Comparison of CBL, RBT and PET Logs in a Test Well with Induced Channels, Society of Petroleum Engineers, 1988.

Allan, M.L., Thermal Conductivity of Cementitious Grouts for Geothermal Heat Pumps: FY 1997 Progress Report, BNL 65129, November, 1997.

Aragon, F., Belmont, J., Parton, H., and Strickland, R., Test Results for Cementitious Grouts in U-Tube Heat Exchangers, Part 2, University of Alabama, Senior Project Report, 1998.

Benny, H.L. and Olson, L.D., Remote Nondestructive Testing of Grouted Radioactive Waste, Concrete International, 1991.

Beck J.V., Cole, K.D., Haji-Sheikh A., and Litkouhi, B., Heat Conduction Using Green's Functions, Hemisphere, 1973

Biot, M.A., The Theory of Propagation of Elastic Waves in a Fluid-Saturated Porous Solid, Journal of Acoustical Society of America, Vol. 28, 1956.

Bruce, D.A., DiMillio, A.F., and Juran, I, A Primer on Micropiles, Civil Engineering, pp. 51-54, December, 1995.

Carslaw, H.S. and Jaeger, J.C., Conduction of Heat in Solids, Claremore Press, Oxford, UK, 1946.

Couvillion, R.J. and Cotton, D.E., Laboratory and Computer Comparisons of Ground-Coupled Heat Pump Backfills, ASHRAE Transactions, 1996.

Eckhart, F., Grouting Procedures for Ground-Source Heat Pump Systems, Oklahoma State University, Ground Source Heat Pump Publications, 1991.

Edil, T.B., Chang, M.M.K., Lan, L.T., and Riewe, T.V., Sealing Characteristics of Selected Grouts for Water Wells, Ground Water, V. 30, No. 3, pp. 351-361, 1992.

Foelich, B., Dumont, A., Pittman, D. and Seeman, B., Cement Evaluation Tool: A New Approach to Cement Evaluation, SPE 1027, Society of Petroleum Engineers, 1982.

Gu, Y. and O'Neal D.L., Modeling the Effect of Backfills on U-Tube Ground Coil Performance, ASHRAE Transactions, 1998.

Gu, Y. and O'Neal D.L., Development of an Equivalent Diameter Expression for Vertical U-Tubes Used in Ground-Coupled Heat Pumps, ASHRAE Transactions, 1998.

Goodwin, K.J. and Carpenter, W.W., Cement Sheath Evaluation, Worldwide Cementing Practices, American Petroleum Institute, 1991.

Haberfield, C.M. and Baycan, S., "Field Performance of the Grout/Rock Interface in Anchors", International Conference on Ground Anchorages and Anchored Structures, Institution of Civil Engineers, London, 20-21 March, 1997.

Hayman, A. J., Gai, H. and Toma, I., A Comparison of Cementation Logging Tools in a Full-Scale Simulator, SPE 22779, Society of Petroleum Engineers, 1991.

Ingersoll, L.R., Zobel, O.J. and Ingersoll, A.C., Heat Conduction with Engineering, Geological and Other Applications, McGraw-Hill, New York, 1954.

Jutten, J.J. and Hayman, A.J., Microannulus Effect on Cementation Logs: Experiments and Case Histories, SPE 25377, Society of Petroleum Engineers, 1993.

Kavanaugh, S.P. and Allan, M.L., Testing of Thermal Enhanced Cement Ground Heat Exchanger Grouts, submitted for ASHRAE Winter Conference, 1999.

Khayat, K.H. and Yahia, A., Effect of Welan Gum-High-Range Water Reducer Combinations on Rheology of Cement Grouts, American Concrete Institute Materials Journal, V. 94, No. 5, 1997.

Kurt, C.E. and Johnson, R.C., "Permeability of Grout Seals Surrounding Thermoplastic Well Casing", Ground Water, V. 20, No. 4, pp. 415-419, 1982.

Lei, T.K., Development of a Computational Model for a Ground-Coupled Heat Exchanger, ASHRAE Transactions, 1993.

Mindess, S. and Young, J.F., Concrete, Prentice-Hall, Englewood Cliffs, 1981.

Neville, A.M., Properties of Concrete, Fourth Edition, John Wiley and Sons, New York, 1996.

Peek, S., Rimel, J., and Suggs, D., Test Results for Cementitious Grouts in U-Tube Heat Exchangers, Part 1, University of Alabama, Senior Project Report, 1997.

Philippacopoulos, A.J., Spectral Green's Dyadic for Point Sources in Poroelastic Media, Journal of Engineering Mechanics, ASCE, 1998.

Philippacopoulos, A.J., Buried Point Source in a Poroelastic Halfspace, Journal of Engineering Mechanics, ASCE, 1997.

Rens, K.L., Wipf, T.J. and Klaiber, F.W., Review of Nondestructive Evaluation Techniques of Civil Infrastructure, Journal of Performance of Constructed Facilities, ASCE, 1997.

Rens, K.L., Wipf, T.J. and Klaiber, F.W., Literature Review: NDT of Civil Engineering Structures, Report R-853, Association of American Railroads, Chicago, Il., 1993.

Remund, C.P. and Lund, J.T., Thermal Enhancement of Bentonite Grouts for Vertical GSHP Systems, in Heat Pump and Refrigeration Systems, K.R. Den Braven and V. Mei (Eds.), American Society of Mechanical Engineers, 29, pp. 95-106, 1993.

Roberts, A. Geotechnology, Pergamon Press, Exeter, 1977.

Rottmayer, S., Beckman, W. and Mitchell, J., Simulation of a Single Vertical U-Tube Ground Heat Exchanger in an Infinite Medium, ASHRAE Transactions, 1997.

Serra, O., Fundamental of Well-Log Interpretation, Elsevier, Amsterdam, 1984.

Sheives, T.C. et al., A Comparison of New Ultrasonic Cement and Casing Evaluation Logs with Standard Cement Bond Logs, SPE 15436, Society of Petroleum Engineers, 1986.

Skaggs, C.B., Rakitsky, W.G., and Whitaker, S.F., Applications of Rheological Modifiers and Superplasticizers in Cementitious Systems, in Fourth CANMET/ACI International Conference on Superplasticizers and Other Chemical Admixtures in Concrete, American Concrete Institute SP 148, Detroit, 1994.

Sommer, F.S. and Jenkins, D.P., Channel Detection Using Pulsed Neutron Logging in a Borax Solution, SPE 25383, Society of Petroleum Engineers, 1993.

Su, D.W-H. and Cotton, S.A., Verification of a Seismic Tomogram Interpretation by Finite Element Analysis, Rock Mechanics, Tillerson & Wawersik (eds), Balkema, Rotterdam, 1990.